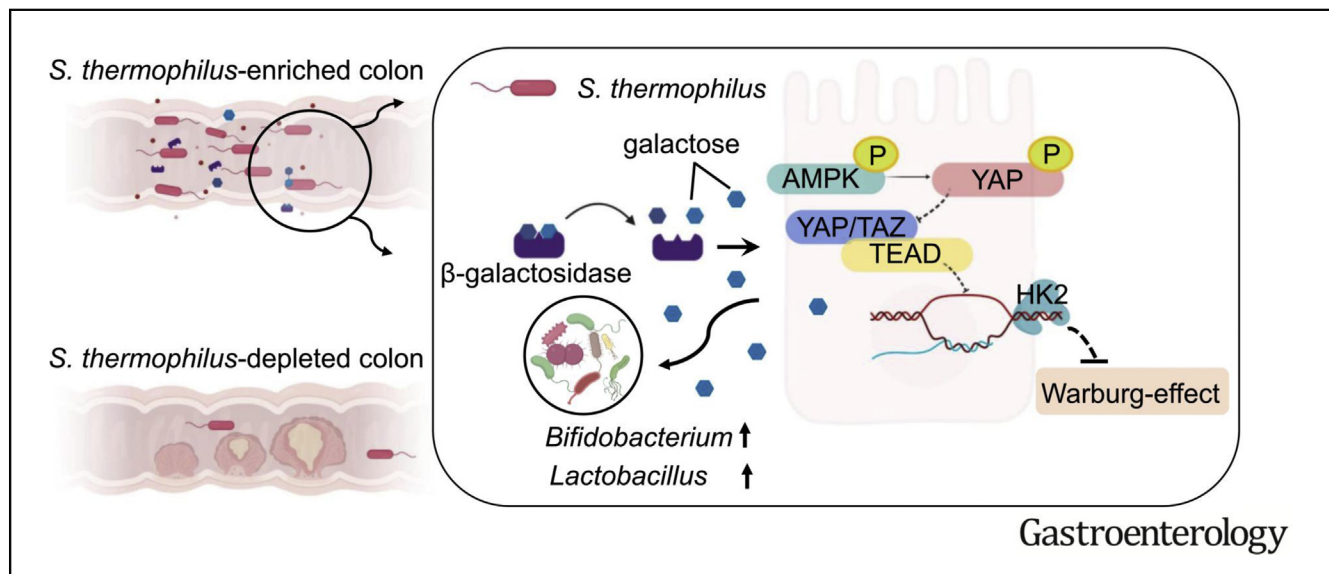




Streptococcus thermophilus Inhibits Colorectal Tumorigenesis Through Secreting β -Galactosidase

Qing Li,^{1,2} Wei Hu,¹ Wei-Xin Liu,^{2,3} Liu-Yang Zhao,^{2,3} Dan Huang,¹ Xiao-Dong Liu,¹ Hung Chan,¹ Yuchen Zhang,¹ Ju-Deng Zeng,¹ Olabisi Oluwabukola Coker,^{2,3} Wei Kang,⁴ Simon Siu Man Ng,⁵ Lin Zhang,^{1,2} Sunny Hei Wong,^{2,3} Tony Gin,¹ Matthew Tak Vai Chan,^{1,*} Jian-Lin Wu,^{6,*} Jun Yu,^{2,3,*} and William Ka Kei Wu^{1,2,*}

¹Department of Anaesthesia and Intensive Care and Peter Hung Pain Research Institute, The Chinese University of Hong Kong, Hong Kong, China; ²State Key Laboratory of Digestive Diseases, Li Ka Shing Institute of Health Sciences, The Chinese University of Hong Kong, Hong Kong, China; ³Department of Medicine and Therapeutics, The Chinese University of Hong Kong, Hong Kong, Hong Kong, China; ⁴Department of Anatomical and Cellular Pathology, The Chinese University of Hong Kong, Hong Kong, Hong Kong, China; ⁵Department of Surgery, The Chinese University of Hong Kong, Hong Kong, China; and ⁶State Key Laboratory of Quality Research in Chinese Medicines, Macau University of Science and Technology, Taipa, Macao



BACKGROUND & AIMS: *Streptococcus thermophilus* was identified to be depleted in patients with colorectal cancer (CRC) by shotgun metagenomic sequencing of 526 multcohorts fecal samples. Here, we aim to investigate whether this bacterium could act as a prophylactic for CRC prevention. **METHODS:** The antitumor effects of *S thermophilus* were assessed in cultured colonic epithelial cells and in 2 murine models of intestinal tumorigenesis. The tumor-suppressive protein produced by *S thermophilus* was identified by mass spectrometry and followed by β -galactosidase activity assay. The mutant strain of *S thermophilus* was constructed by homologous recombination. The effect of *S thermophilus* on the gut microbiota composition was assessed by shotgun metagenomic sequencing. **RESULTS:** Oral gavage of *S thermophilus* significantly reduced tumor formation in both *Apc*^{min/+} and azoxymethane-injected mice. Coincubation with *S thermophilus* or its conditioned medium decreased the proliferation of cultured CRC cells. β -

Galactosidase was identified as the critical protein produced by *S thermophilus* by mass spectrometry screening and β -galactosidase activity assay. β -Galactosidase secreted by *S thermophilus* inhibited cell proliferation, lowered colony formation, induced cell cycle arrest, and promoted apoptosis of cultured CRC cells and retarded the growth of CRC xenograft. The mutant *S thermophilus* without functional β -galactosidase lost its tumor-suppressive effect. Also, *S thermophilus* increased the gut abundance of known probiotics, including *Bifidobacterium* and *Lactobacillus* via β -galactosidase. β -Galactosidase-dependent production of galactose interfered with energy homeostasis to activate oxidative phosphorylation and downregulate the Hippo pathway kinases, which partially mediated the anticancer effects of *S thermophilus*. **CONCLUSION:** *S thermophilus* is a novel prophylactic for CRC prevention in mice. The tumor-suppressive effect of *S thermophilus* is mediated at least by the secretion of β -galactosidase.

Keywords: *S thermophilus*; colorectal cancer; β -galactosidase.

Colorectal cancer (CRC) is the third most common cancer and the fourth leading cause of cancer death globally.¹ The long stepwise progression of CRC from cellular transformation to full-blown metastatic lesions has enabled its prevention through natural compounds or drugs to block this process. In particular, economic analysis suggests that chemoprevention could be a cost-effective intervention when targeted at intermediate-risk populations after polypectomy.² To this end, nonsteroidal anti-inflammatory drugs and cyclooxygenase 2 inhibitors have been shown to reduce the occurrence of CRC or its precancerous lesions in high-risk individuals.³ However, the long-term use of these agents has been associated with an increased risk of cardiovascular events, posing the concern of a high risk-to-benefit ratio for recommending these agents for CRC chemoprevention. New prevention strategies for CRC without significant adverse effects are therefore highly warranted.

The association of CRC with altered gut microbiota has been studied in different populations, identifying CRC-enriched bacteria such as *Fusobacterium nucleatum*, *Pectostreptococcus stomatis*, *Pectostreptococcus anaerobius*, and *Bacteroides fragilis* that may be important in intestinal tumorigenesis.⁴ On the other hand, the direct evidence supporting the use of CRC-depleted probiotics as a kind of prophylactic for preventing CRC is lacking. Nevertheless, the potential cancer-preventing effects of probiotics (the health-promoting bacteria) have been sporadically reported in animal models, cell line models, and clinical trials.

Probiotics were also reported to play a protective role in reducing the intestinal inflammation, repairing the intestinal barrier, and restraining the development of CRC.⁵ In this regard, probiotics may help lower the risk of CRC. We have demonstrated that *Streptococcus thermophilus* is depleted in CRC patients' gut compared with healthy controls.⁶ *Streptococcus thermophilus* is a gram-positive, fermentative, facultative anaerobe. It is generally used in yogurt production and can be found in fermented milk products. This organism has been shown to protect the gastrointestinal epithelium from enteroinvasive *Escherichia coli*, improve somatic growth in infants, and reduce the severity and duration of acute diarrhea in young infants.^{7,8} More recently, *S thermophilus* has been reported to diminish the severity of methotrexate-induced small-intestinal mucositis in rats.⁹ However, the role of *S thermophilus* in CRC has not been defined.

In this study, we elucidated the functional role of *S thermophilus* in preventing intestinal tumorigenesis in vitro and in vivo and explored the mechanisms of its protective effect against CRC development. We revealed that *S thermophilus* prevented CRC development by secreting β -galactosidase.

WHAT YOU NEED TO KNOW

BACKGROUND AND CONTEXT

Streptococcus thermophilus was found to be depleted in patients with colorectal cancer (CRC). We investigated if this bacterium could act as a prophylactic for CRC prevention.

NEW FINDINGS

S thermophilus suppressed intestinal tumorigenesis in mice. The tumor-suppressive effect of *S thermophilus* was mediated, at least in part, by the secretion of β -galactosidase.

LIMITATIONS

This study was performed with cell lines, human fecal samples, and mouse models of CRC; additional interventional studies are needed in humans.

IMPACT

This probiotic could be used as a potential prophylactic for preventing CRC in humans with minimal side effects.

Materials and Methods

Bacterial Strain and Culture Condition

Streptococcus salivarius (2593) and *S thermophilus* (19258) were purchased from the American Tissue Culture Collection (ATCC, Manassas, VA). *Bacillus halodurans* (DSM 18197) was obtained from Deutsche Sammlung von Mikroorganismen und Zellkulturen GmbH (Braunschweig, Germany). They were cultured in Brain Heart Infusion (BHI) broth (CM1135B; Thermo Fisher Scientific, West Palm Beach, FL) for 24 hours at 37°C in aerobic conditions. A nonpathogenic human commensal intestinal bacterium, *E coli* strain MG1655, was used as a bacterial control and was cultured in the same condition as *S thermophilus*. When the density of *S thermophilus* reached an optical density 600 (OD₆₀₀) of 0.5, the bacteria culture medium was centrifuged at 4500g for 15 minutes and filtered through a 0.2- μ m pore-size filter to obtain the *S thermophilus* conditioned medium (St.CM). The prepared St.CM was separated with a molecular weight cutoff spin column (Merck KGaA, Darmstadt, Germany). The >100-kDa fraction was obtained by centrifuging the conditioned-medium through a 100,000 nominal molecular weight limit membrane.

* Authors are co-corresponding authors.

Abbreviations used: in this paper: ACC, acetyl-CoA carboxylase; AMPK, adenosine 5'-monophosphate-activated protein kinase; AOM, azoxymethane; ATCC, American Tissue Culture Collection; BHI, Brain Heart Infusion; CFU, colony forming units; CM, conditioned medium; CRC, colorectal cancer; DMEM, Dulbecco's modified Eagle medium; FBS, fetal bovine serum; HK2, hexokinase 2; mRNA, messenger RNA; MTT, 3-(4,5-Dimethylthiazol-2-yl)-2,5-diphenyltetrazolium bromide; OCR, oxygen consumption rate; OD, optical density; OXPHO, oxidative phosphorylation; PBS, phosphate-buffered saline; PCR, polymerase chain reaction; PK, protease K; St.CM, conditioned medium of *Streptococcus thermophilus*; TAZ, transcriptional coactivator with PDZ-building motif; WT, wild-type; YAP, yes-associated protein.

 Most current article

© 2021 by the AGA Institute
0016-5085/\$36.00

<https://doi.org/10.1053/j.gastro.2020.09.003>

Streptococcus thermophilus Mutant Strain Construction

The mutant *S thermophilus* (*LacZ* knockout) was constructed by homologous recombination. Kanamycin resistance gene fragment was amplified from the pCR2.1-TOPO plasmid. Sequences around 1-kilobase (kb) upstream and downstream with 500-base pair space were amplified from the genomic DNA of *S thermophilus*, respectively. Subsequently, 3 DNA fragments, including the sequences around 1-kb upstream of the *LacZ* gene encoding β-galactosidase and 900-base pair kanamycin-resistance gene, and sequences around 1-kb downstream of the *LacZ* gene, were cleaved by restriction enzymes and then linked successively. The recombinant DNA fragment was linked into the pCR2.1-TOPO plasmid using the thymine-adenine cloning technique. The recombinant pCR2.1-TOPO plasmid was transformed into the competent cells of *S thermophilus* by electroporation (1.8 kV, 200 Ω, and 25 μF). The competent cell was constructed by exposing *S thermophilus* to 50 mL BHI broth containing 20 mmol/L DL-threonine for 2 to 2.5 hours to reach an OD₆₀₀ of 0.2 to 0.3. The cells pellets (4500g, 15 minutes) were washed with 5 mL electroporation buffer (7 mmol/L HEPES and 1 mmol/L MgCl₂, pH 6.0) and resuspended to an OD₆₀₀ of 20 in the same buffer to obtain the electrocompetent cells. The electroporated cells were spread onto prewarmed BHI agar plates containing X-gal, and the representative putative transformant colonies were then cultured in selective antibiotic (50 μg/mL kanamycin) for genomic isolation and β-galactosidase activity test. The presence of the relevant plasmid species was confirmed by agarose gel electrophoresis examination.

Cell Culture

CRC cell lines, namely, HCT116, HT29, and Caco-2, were obtained from the ATCC. Human normal colon epithelial cell line NCM460 was obtained from INCELL Corporation (San Antonio, TX). All of the cell lines were grown in high-glucose Dulbecco's Modified Eagle's Medium (DMEM) (Gibco BRL, Grand Island, NY) supplemented with 10% (vol/vol) fetal bovine serum (FBS), and 1% penicillin/streptomycin in a humidified atmosphere containing 5% CO₂. For yes-associated protein 1 (YAP1)-HCT116 cell line establishment, pcDNA3.1(+)/YAP1 and empty vector were transfected into HCT116 cells to get the YAP1-overexpressed cell line, and the clones that stably expressed YAP1 were selected as mentioned before.¹⁰

Cell Viability Assay

Cell viability was determined by the 3-(4,5-dimethylthiazol-2-yl)-2,5-diphenyltetrazolium (MTT) assay. For each well in the 96-well plate, 1000 cells were seeded and treated with the bacteria-conditioned medium or bacteria directly. For coculture of bacteria and eukaryotic cells, the penicillin/streptomycin in the culture medium was removed, and cells were exposed to bacteria with multiplicity of infection of 100 for 4 hours in aerobic conditions. Afterward, the medium containing bacteria was replaced by DMEM supplemented with 10% FBS, 1% penicillin/streptomycin, and 50 μg/mL gentamycin for 2 hours, which was used to kill all of the extracellular bacteria. The medium containing the killed bacteria body and debris was

replaced by DMEM supplemented with 10% FBS and 1% penicillin/streptomycin for further experiments.

Carcinogen-Induced Cancer Model

For these experiments, 6-week-old male conventional C57BL/6 wild-type (WT) mice underwent 6 consecutive intraperitoneal injections of azoxymethane (AOM; 10 mg/kg) at 1-week intervals, followed by administration of 1 × 10⁸ colony forming units (CFU) of *S thermophilus*, *E coli* MG1655, or the same volume of phosphate-buffered saline (PBS) every day for 20 weeks for the development of neoplastic lesions. Sulindac (180 ppm/wk) was used as a positive control.

Adenomatous polyposis coli/Multiple Intestinal Neoplasia Colorectal Cancer Model

C57BL/6J-*Apc*^{Min/+} mice, which harbor a germline mutation in the tumor suppressor gene *Apc* and develop intestinal polyps spontaneously, were purchased from The Jackson Laboratory (Bar Harbor, ME) and maintained in the animal facility at the Chinese University of Hong Kong. Genotyping was conducted by routine allele-specific polymerase chain reaction (PCR) assay. The same treatment with the AOM model was used in 6-week-old male *Apc*^{min/+} mice, and they were raised until 20 weeks for the evaluation of the bacteria treatment efficacy. All experimental procedures were approved by the Chinese University of Hong Kong Animal Ethics Committee.

Statistical Analysis

Data are expressed as mean ± SD. The independent Student *t* test or Mann-Whitney *U* test was used to compare the difference between the 2 groups where appropriate. One-way analysis of variance was used to compare the difference between multiple groups. The difference in cell viability was determined by 2-way analysis of variance. Pathway enrichment analysis was conducted by Kyoto Encyclopedia of Genes and Genomes database. Differences with *P* < .05 were considered statistically significant. All tests were performed using GraphPad Prism 8.0 software (GraphPad Software, San Diego, CA).

Additional methods are provided in the [Supplementary Material](#).

Results

Streptococcus thermophilus Is Depleted in Stool Samples of Patients With Colorectal Cancer

Our previous shotgun metagenomic sequencing showed that there were 62 depleted bacteria species in CRC patients compared with normal individuals.⁶ We reanalyzed the top 20 depleted strains with the largest fold change and found that *S salivarius* and *S thermophilus* were 2 known probiotics ([Supplementary Figure 1A](#)). To determine the effect of the most significantly CRC-depleted *S salivarius* on intestinal tumorigenesis, we gavaged *Apc*^{min/+} mice with *S salivarius* (1 × 10⁸ CFU/d) for 8 weeks. Two other experimental groups—gavaged with nontumorigenic intestinal microflora *E coli* strain MG1655 (1 × 10⁸ CFU/d) or PBS—were used as control. Unfortunately, the tumor number and tumor load in the colon and the small

intestine were not significantly different between the *S salivarius* group and the 2 control groups (*Supplementary Figure 2*).

We next moved to the second CRC-depleted probiotic, namely *S thermophilus*. The association between *S thermophilus* and CRC was verified by quantitative PCR in 78 CRC and 78 normal stool samples. As shown in *Supplementary Figure 1B*, *S thermophilus* was significantly depleted in stool samples of patients with CRC compared with normal controls. Such depletion was further confirmed with our in-house fecal shotgun metagenomic data from 202 healthy control individuals and 183 CRC patients (*Supplementary Figure 1C*).

Streptococcus thermophilus Protects Against Intestinal Tumorigenesis in 2 Murine Models of Colorectal Cancer

Mouse experiments were then conducted to evaluate the potential protective effect of *S thermophilus* in CRC. Six-week-old *Apc*^{min/+} mice were orally gavaged with *S thermophilus* (1×10^8 CFU/200 μ L/d) or *E coli* strain MG1655 (1×10^8 CFU/200 μ L/day, control) for 14 consecutive weeks. Sulindac (180 ppm every 3 days), a nonsteroidal anti-inflammatory drug that has been reported to protect against CRC,¹¹ was used as a positive control. *S thermophilus*-gavaged mice had an obvious reduction in tumor number and size (*Figure 1A* and *C*) compared with those gavaged with the *E coli* strain MG1655 or the PBS. Sulindac, as expected, inhibited CRC development. The tumor histology was further examined (*Figure 1B*), and the levels of *S thermophilus* in stool were confirmed to be increased significantly after administration of *S thermophilus* by oral gavage (*Supplementary Figure 3C*). The mouse body weight and the incidence of CRC-related conditions (ie, bloody stool and rectocele), however, were not significantly altered in *S thermophilus*-gavaged mice (*Supplementary Figure 3A* and *B*).

The tumor-suppressive effect of *S thermophilus* was further validated in a carcinogen-induced CRC model in which 6-week-old C57BL/6 mice were injected with the carcinogen AOM (10 mg/kg) once a week for 6 weeks, followed by oral administration of *S thermophilus* for 20 weeks. We observed consistent results as in the *Apc*^{min/+} mice (*Figure 1D–F*, *Supplementary Figure 3D–F*).

Streptococcus thermophilus and Its Conditioned Medium Inhibit the Viability of Colon Cancer Cells

We next determined whether *S thermophilus* had a direct antitumorigenic effect in vitro. Colon cancer cell lines HCT116, HT29, and Caco-2, and colon normal epithelial cell line NCM460 were cocultured without or with *S thermophilus* (multiplicity of infection = 100) for 4 hours. *E coli* strain MG1655 and PBS were used as bacterial and blank controls, respectively. As shown in *Figure 1G*, coculture with *S thermophilus* caused a significant decrease in cell viability of colon cancer cell lines but not the normal epithelial cells.

These results indicate that *S thermophilus* preferentially inhibited CRC cell viability.

We next explored whether such function was attributed to *S thermophilus* itself or its secreted products. Live *S thermophilus* was heat-killed by autoclaving and subsequently exposed to colon cells. As shown in *Supplementary Figure 4A*, reduction of colon cancer cell viability was not observed upon exposure to heat-killed *S thermophilus*.

In another set of experiments, a transwell insert with 0.44- μ m pores was used. Live *S thermophilus* or *E coli* was seeded into the insert and only its metabolites were allowed to diffuse through the pores to contact the host cells. A significant reduction of colon cancer cell viability was observed (*Supplementary Figure 4B*). Furthermore, all bacteria bodies and debris in the live bacterial culture supernatant were removed by centrifugation and filtration through a 0.22- μ m membrane to obtain the CM that was used to treat HCT116, HT29, Caco-2, and NCM460 cells at the concentration of 12.5% (vol/vol) for 4 consecutive days. MTT assays indicated that St.CM suppressed the viability of colon cancer cells but not normal colon epithelial cells in a time-dependent manner (*Figure 2A*), indicating that the antitumor effect of *S thermophilus* was mainly caused by the bacteria-secreted molecules.

Streptococcus thermophilus Conditioned Medium (>100-kDa) Induces Apoptosis and Growth 0/1-Phase Cell Cycle Arrest of Colorectal Cancer Cells and Retards Colorectal Cancer Cells Xenograft Growth

To identify the secreted molecule(s) responsible for the tumor-suppressive effect of *S thermophilus*, we separated St.CM into 2 molecular-weight fractions using 100-kDa molecular weight cutoff membranes. The cells were then exposed to >100-kDa fraction or <100-kDa fraction (1% vol/vol) for 24 hours, respectively. As shown in *Figure 2B*, the >100-kDa fraction of St.CM lowered the viability of colon cancer cells, whereas the <100-kDa fraction failed to produce any significant effect.

This growth-inhibitory effect was further confirmed by colony formation assay, proliferating cell nuclear antigen protein levels, and Ki-67 immunostaining (*Figure 2C–E*). These results suggested that the molecules >100-kDa in St.CM mediated the tumor-suppressive effect. Moreover, cells treated with the St.CM >100-kDa fraction showed an increase in apoptosis (*Figure 2F*). Treatment with St.CM >100-kDa fraction also decreased the proportion of cells in the synthesis (S) and growth (G)₂ phases and increased G₀/G₁-phase cells in HCT116 and HT29 (*Figure 2G*).

The function of St.CM >100-kDa fraction on the growth of CRC xenografts in nude mice was further examined. After intratumoral administration of the St.CM >100-kDa fraction, the xenograft growth rate was significantly lowered than those treated with the BHI >100-kDa, BHI <100-kDa, or St.CM <100-kDa fractions (*Figure 2H*).

Characterization of the *Streptococcus thermophilus*-Secreted Tumor-Suppressive Molecule(s)

We further characterized the antitumor molecule(s) in the St.CM >100-kDa fraction with or without digestion by protease K (PK, 50 µg/mL). As shown in Figure 3A, the inhibitory effect of St.CM >100-kDa fraction existed in the non-PK-digested group but not in the PK-treated group, indicating that the antitumor molecule(s) in the St.CM >100-kDa fraction were protein. Consistently, heating the St.CM >100-kDa fraction to 100°C for 30 minutes abrogated its tumor-suppressive action (Figure 3B).

The potential functional secreted proteins were then separated by 5% sodium dodecyl sulfate-polyacrylamide gel electrophoresis and acquired by in-gel digestion, which was then analyzed by mass spectrometry. The 2-dimensional nano-scale liquid chromatography-quadrupole time-of-flight tandem-mass spectrometry results suggested that β-galactosidase (Figure 3C, Supplementary Figure 5) was markedly enriched in the St.CM >100-kDa fraction. The amount of β-galactosidase and its activity in the St.CM >100-kDa fraction was also significantly higher than that of the *E. coli* CM >100-kDa, BHI >100-kDa, BHI <100-kDa, and St.CM <100-kDa fractions (Figure 3D). These results indicated that an anti-tumor fraction separated from the St.CM contained a large amount of β-galactosidase.

The Antitumor Effect of *Streptococcus thermophilus* Is Mediated by the Secretion of β-Galactosidase

To determine the functional involvement of β-galactosidase, we constructed a mutant *S. thermophilus* strain (*LacZ* knockout) by homologous recombination (Supplementary Figure 6A). The successful insertion of the kanamycin-resistance gene to *LacZ* (the gene encoding β-galactosidase), which was confirmed by PCR and blue-white screen (Supplementary Figure 6B), functionally abolished the β-galactosidase activity (Supplementary Figure 6C). 16S ribosomal RNA gene sequencing further confirmed the mutant strain as *S. thermophilus* (Supplementary Figure 6D).

To assess the effect of mutant *S. thermophilus* on cell viability, colon cell lines and human CRC organoids were exposed to the St.CM with the *LacZ* gene knocked out (St.CM-KO). We found that the tumor-suppressive effect was lost after knocking out the *LacZ* gene (Figure 4A and B). Furthermore, gavage of *LacZ*-knockout *S. thermophilus* into *Apc*^{min/+} mice failed to protect against intestinal tumorigenesis (Figure 4C and D). The overall β-galactosidase activity was also confirmed to be increased significantly in stools of WT mice administered *S. thermophilus*, while no such changes were observed in the stools of mice receiving the mutant *S. thermophilus* (Figure 4E). These findings suggest that the antitumor effect of *S. thermophilus* was mediated by the secretion of β-galactosidase.

To determine the effect of *S. thermophilus* inoculation on the gut microbiota composition, shotgun metagenomic sequencing of fecal samples from the *Apc*^{min/+} mouse model was performed. Daily administration of *S. thermophilus*

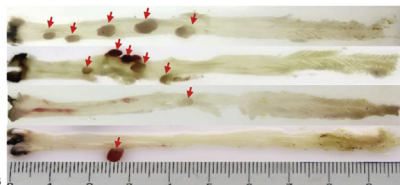
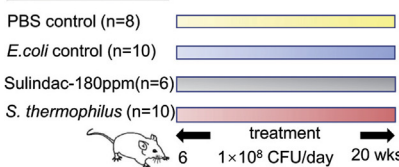
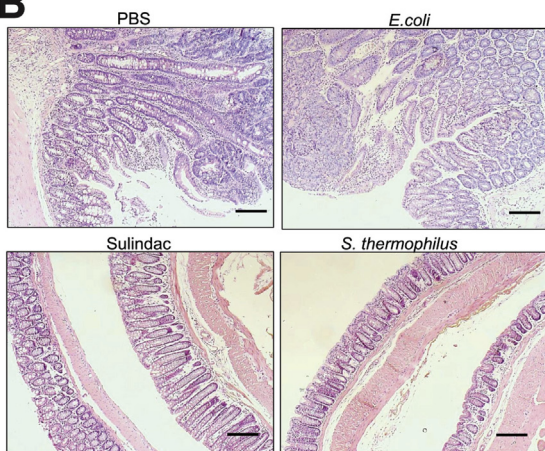
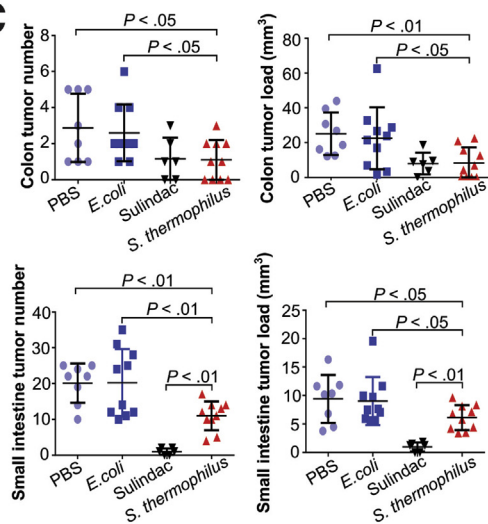
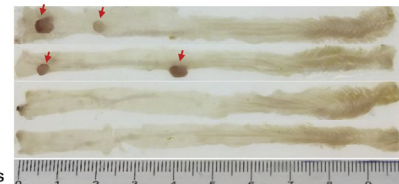
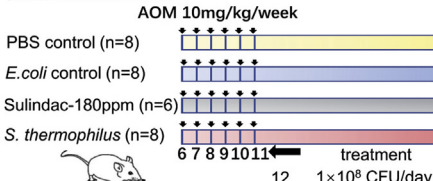
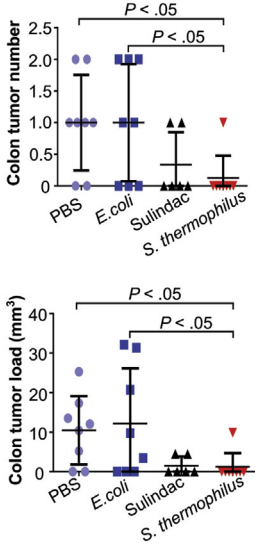
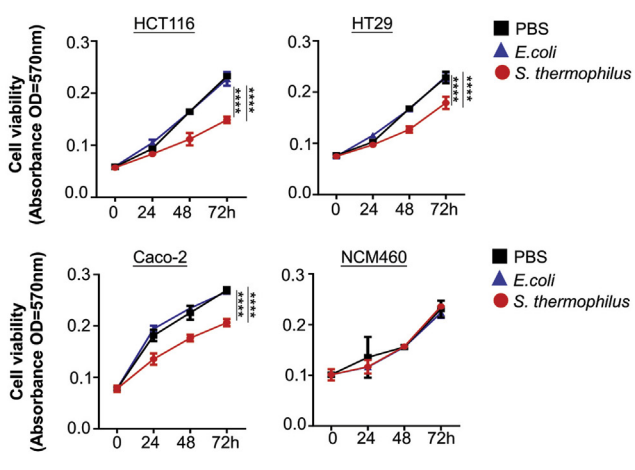
caused pervasive compositional alterations of the gut microbiota as revealed by principal coordinate analysis (Figure 4F). The relative abundance of bacteria at the phylum level revealed a reduction of Firmicutes and an increase in Actinobacteria in *S. thermophilus*-gavaged mice (Supplementary Figure 7A). Notably, *S. thermophilus* administration caused enrichment of the probiotic *Bifidobacterium* and *Lactobacillus* genera, including *B. choerinum*, *B. pseudolongum*, *B. coryneforme*, *Lactobacillus reuteri*, *L. animalis*, and *L. acidophilus*. In addition, the previously reported CRC-depleted bacteria *L. gallinarum*⁶ also showed a significant increase. All of these changes were dependent on β-galactosidase because the knockout strain failed to produce such alterations (Figure 4G). Besides, we identified 14 bacteria whose alterations by *S. thermophilus* were independent of β-galactosidase (Supplementary Figure 7B).

We also determined in vivo colonization of *S. thermophilus* with both fecal and mucosal samples. We observed that the abundance of *S. thermophilus* was markedly elevated in fecal samples of mice receiving both WT and mutant *S. thermophilus*. It is worth noting that the fecal abundance of the mutant *S. thermophilus* was lower than that of the WT strain (Supplementary Figure 7C), suggesting that β-galactosidase could play a role in the in vivo colonizing ability of *S. thermophilus*. No colonization of *S. thermophilus*, regardless of the β-galactosidase status, on the mouse mucosa could be detected (Supplementary Figure 7D). Besides, the in vitro attachment assay revealed that the WT and mutant *S. thermophilus* both had no ability to attach on the colon cancer cells (Supplementary Figure 7E).

We further isolated the *S. thermophilus* LL23 strain from the fecal sample of normal healthy individuals (Supplementary Figure 8A) to assess whether a strain-dependent effect of *S. thermophilus* on CRC exists. We determined the β-galactosidase activity from the LL23 strain and found that the level of β-galactosidase from the LL23 strain was lower than that in the ATCC *S. thermophilus* strain (Supplementary Figure 8B).

We then treated the colon cells with the CM of LL23 (LL23.CM) at the concentration of 15% for 4 consecutive days. MTT assay suggested that LL23.CM similarly suppressed the viability of cancer cells but not the normal colon epithelial cells (Supplementary Figure 8C). LL23 could also reduce the tumor number in the intestine of *Apc*^{min/+} mice (Figure 4H and I). However, the tumor size was not significantly changed in the LL23-treated mice (Supplementary Figure 9), suggesting the intraspecies heterogeneity of β-galactosidase activity might affect the CRC-suppressive effect of *S. thermophilus*.

Because β-galactosidase can be produced by a large repertoire of bacteria, we further assessed whether β-galactosidase derived from the *E. coli* overproducer could exert similar a tumor-suppressive effect. Intriguingly, the β-galactosidase in the St.CM >100-kDa fraction remained active throughout the reaction, whereas the activity of *E. coli*-derived β-galactosidase decreased over time (Supplementary Figure 10A), suggesting the β-galactosidase from the *E. coli* overproducer was not stable. Concordantly, we did not observe any inhibitory effect from the

A***Apc* $^{min/+}$ mice****B****C****D*****C57BL/6* mice****E****F****G**

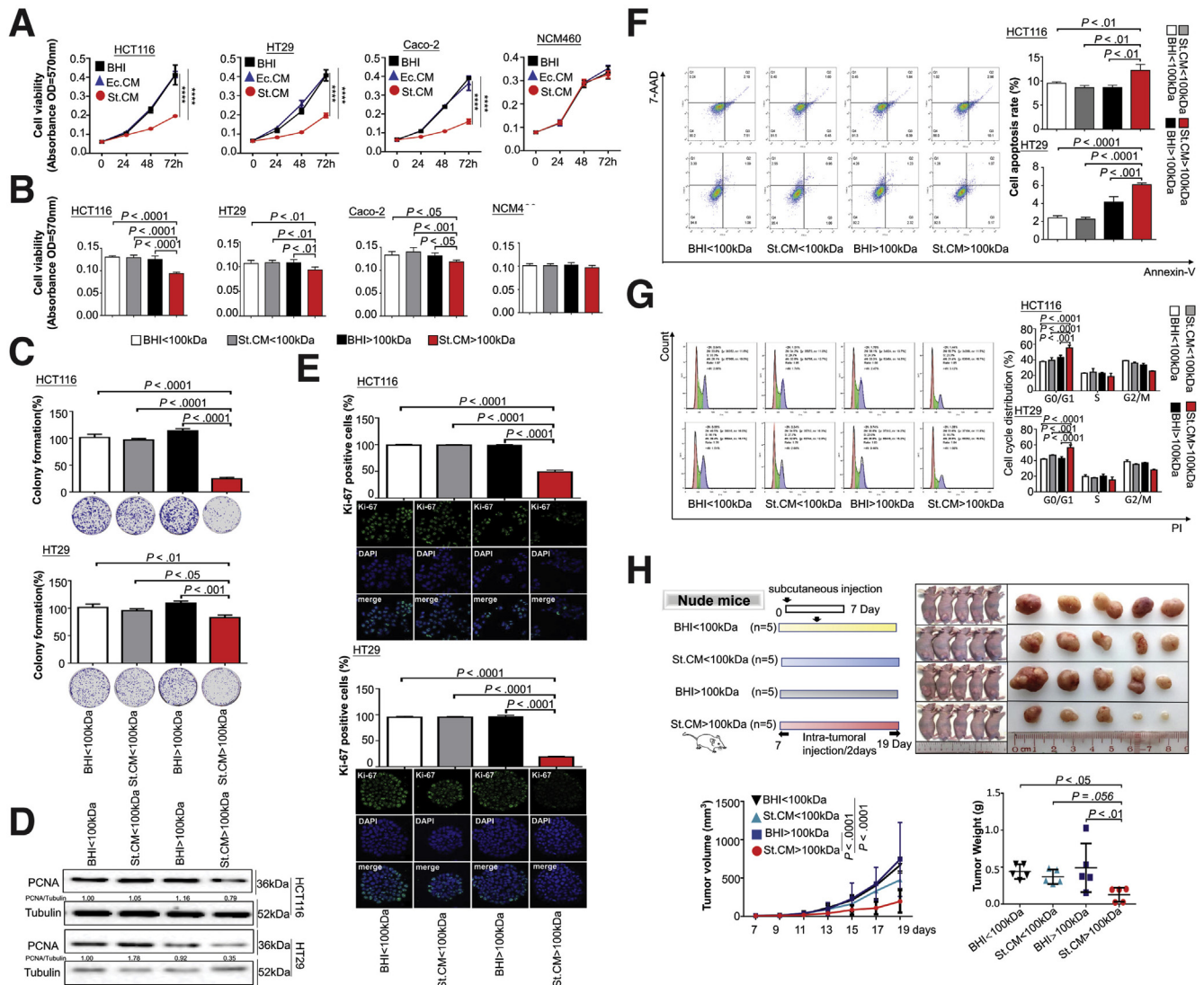


Figure 2. St.CM and St.CM >100-kDa fraction exhibit tumor-suppressive effects in vitro and in vivo. (A) St.CM (12.5%) reduced the colonic cell viability, except NCM460. *Escherichia coli* conditioned medium (Ec.CM) and BHI were used as control. (B) St.CM >100-kDa fraction reduced the CRC cell viability, except normal epithelial cells. (C) St.CM >100-kDa fraction suppressed the colony formation of CRC cells. (D) St.CM >100-kDa fraction reduced proliferating cell nuclear antigen (PCNA) levels in CRC cells. (E) St.CM >100-kDa fraction reduced CRC cell Ki-67 expression levels. (F) St.CM >100-kDa fraction increased CRC cell apoptosis. (G) St.CM >100-kDa fraction induced CRC cell cycle arrest at growth (G₁)/Synthesis (S) phase. (H) St.CM >100-kDa fraction suppressed tumor growth in the xenograft model. Data are expressed as mean \pm SD. Statistical significance was determined by 1-way or 2-way analysis of variance, where appropriate. ***P < .0001.

E. coli-derived β -galactosidase (Supplementary Figure 10B). We also gavaged *Apc*^{min/+} mice with a β -galactosidase-producing bacteria, namely *B. halodurans*, to determine whether β -galactosidase from other bacteria could prevent

CRC. Unfortunately, both the tumor number (Figure 4H and I) and tumor load (Supplementary Figure 9) in the colon and the small intestine were not significantly different between the *B. halodurans* group and the control groups,

Figure 1. *Streptococcus thermophilus* reduces intestinal tumorigenicity in mice. (A) Schematic diagram shows the experimental design, time line, and representative colonic morphologies of the *Apc*^{min/+} mouse model. (B) Representative H&E-stained histologic images of colon tissues from *Apc*^{min/+} mice. Scale bar = 100 μ m. (C) Colonic (upper 2 panels) and small-intestine (lower 2 panels) tumor number and tumor load of *Apc*^{min/+} mice. (D) Schematic diagram shows the experimental design, time line, and representative colonic morphologies of the AOM-induced CRC mouse model. (E) Representative H&E-stained histologic images of colon tissues from AOM-induced CRC mice model. Scale bar = 100 μ m. (F) Colonic tumor number and tumor load of AOM-induced CRC mice model. (G) *Streptococcus thermophilus* (multiplicity of infection = 100) inhibits the cell viability of colon cancer cells HCT116, HT29, and Caco-2 but not the normal colon epithelial cells NCM460, as determined by MTT assay. *Escherichia coli* and PBS were used as control. Results are presented as mean \pm SD. Statistical significance was determined by 1-way or 2-way analysis of variance, where appropriate. ***P < .0001.

indicating the β -galactosidase from other bacteria species may not have an antitumor effect.

The In Vitro and In Vivo Inhibitory Effects of Galactose on Colon Cancer

β -Galactosidase from *S. thermophilus* is known to only metabolize the glucose moiety of lactose, while secreting the galactose without fermentation. We evaluated whether the inhibitory effect of β -galactosidase is associated with the production of galactose. The galactose-to-lactose ratio was increased significantly in the medium of the St.CM >100-kDa fraction-treated cells (Figure 5A) or in cell-free conditions (Figure 5B). These results suggest that β -galactosidase in the St.CM >100-kDa fraction might convert lactose in the cell culture medium into galactose to inhibit the viability of CRC cells. To confirm this finding, CRC cells were exposed to galactose. As shown in Figure 5C, cell viability decreased substantially in HCT116 and HT29 compared with the control group.

Because galactose is mainly absorbed in the small intestine, we therefore gave the mice galactose in drinking water ad libitum for 14 weeks. Consistently, administration of galactose (0.4 mg/mL) decreased small-intestine tumor number in *Apc*^{min/+} mice. However, no significant tumor-suppressive effect of the galactose was observed in the colon, suggesting that the luminal concentrations of galactose are important (Figure 5D). In contrast, *S. thermophilus*-dependent secretion of β -galactosidase is expected to maintain high galactose content throughout the gastrointestinal tract. Consistently, the galactose content in stool samples of mice administered *S. thermophilus* increased significantly compared with those gavaged with PBS, *E. coli*, or the mutant *S. thermophilus* (Figure 5E).

Fecal samples from galactose-treated *Apc*^{min/+} mice were also profiled by shotgun metagenomic sequencing to determine whether galactose exerted any effect on the gut microbiota. There was a significant overall compositional alteration between the galactose group and the water control group (Figure 5F), including a reduction of Verrucomicrobia and an increase in Bacteroidetes at the phylum level (Figure 5G). In accordance with the modulating effect of β -galactosidase on the gut microbiota, galactose treatment produced a significant enrichment of probiotic *Bifidobacterium* and *Lactobacillus* genera, including *B. choerinum*, *B. gallinarum*, *L. animalis*, *L. johnsonii*, *L. murinus*, *L. reuteri*, *Lactobacillus* sp Koumiss, and *Lactobacillus* sp wkB8. Concordantly, previously reported CRC-enriched pathogenic bacteria,⁶ namely *Parvimonas micra*, *Fusobacterium nucleatum*, and *Alistipes finegoldii*, were notably decreased upon galactose administration (Supplementary Table 1).

To explore whether galactose could restore the CRC-preventive effect of the mutant *S. thermophilus*, *Apc*^{min/+} mice were treated with galactose (0.4 mg/mL in drinking water) concomitant with daily oral administration of the mutant *S. thermophilus*. We observed that complementation of galactose significantly decreased the small-intestine tumor number and tumor load in mice receiving the mutant *S.*

thermophilus (Figure 4H and I, Supplementary Figure 9), indicating that galactose could restore the CRC-preventive effect of the mutant *S. thermophilus*. These results collectively confirmed that the CRC-suppressive effect of *S. thermophilus* was mediated by the β -galactosidase-dependent production of galactose.

The Antitumor Effects of Streptococcus *thermophilus* Conditioned Medium >100-kDa Fraction and Galactose Are Dependent on Yes-Associated Protein

To investigate the mechanism underlying the active compound(s) produced by *S. thermophilus* for CRC prevention, RNA sequencing was performed to assess messenger (m)RNA expression altered by St.CM >100-kDa in HCT116, in which 289 deregulated mRNAs were identified (Supplementary Figure 11A; Supplementary Tables 2 and 3). The Hippo signaling pathway was significantly downregulated upon St.CM >100-kDa treatment (Figure 6A, Supplementary Tables 4 and 5). Concordantly, St.CM >100 kDa and galactose downregulated the mRNA of 3 Hippo mediators, namely YAP, transcriptional coactivator with PDZ-building motif (TAZ), and TEA domain family member 1 (TEAD1) (Figure 6B, Supplementary Figure 11B), and induced YAP Ser 127 phosphorylation (Figure 6C), the major phosphorylation site that promotes YAP translocation from the nucleus to the cytoplasm. In addition, St.CM >100-kDa or galactose treatment decreased the protein levels of YAP/TAZ and the nuclear levels of YAP in both cell lines (Figure 6C, Supplementary Figure 11C). Accordingly, treatment with St.CM >100 kDa and galactose decreased the transcription activity of YAP as revealed by the promoter assay of *CTGF*, a downstream YAP target (Figure 6D).

To investigate the direct link between the Hippo pathway and the tumor-suppressive effect of *S. thermophilus*, we used a Hippo pathway inhibitor, CA3, which has a potent inhibitory effect on YAP/TEAD transcription activity. We observed that CA3 treatment downregulated the level of YAP1. Pharmacologic manipulation of the Hippo pathway using CA3 abolished *S. thermophilus*-induced tumor suppression in vitro and in the xenograft model (Figure 6E and F). In addition, CRC patients with high levels of *S. thermophilus* revealed a significant negative correlation with 7 YAP/TAZ target genes, which have been reported as the best and robust indicator to effectively capture Hippo pathway activity, in The Cancer Genome Atlas cohort¹² (Supplementary Figure 11D). Notably, genetic ablation of *LacZ* in *S. thermophilus* abrogated YAP inhibition (Figure 6G). The disrupted Hippo signaling was also explored in tumor tissues isolated from the WT and mutant *S. thermophilus*-gavaged mice. We observed that compared with tumor tissues from the WT *S. thermophilus*, the expression of YAP/TAZ was not reduced in the tumor tissues of mice receiving mutant *S. thermophilus* (Figure 6H), suggesting that β -galactosidase mediated the inhibition of Hippo pathway.

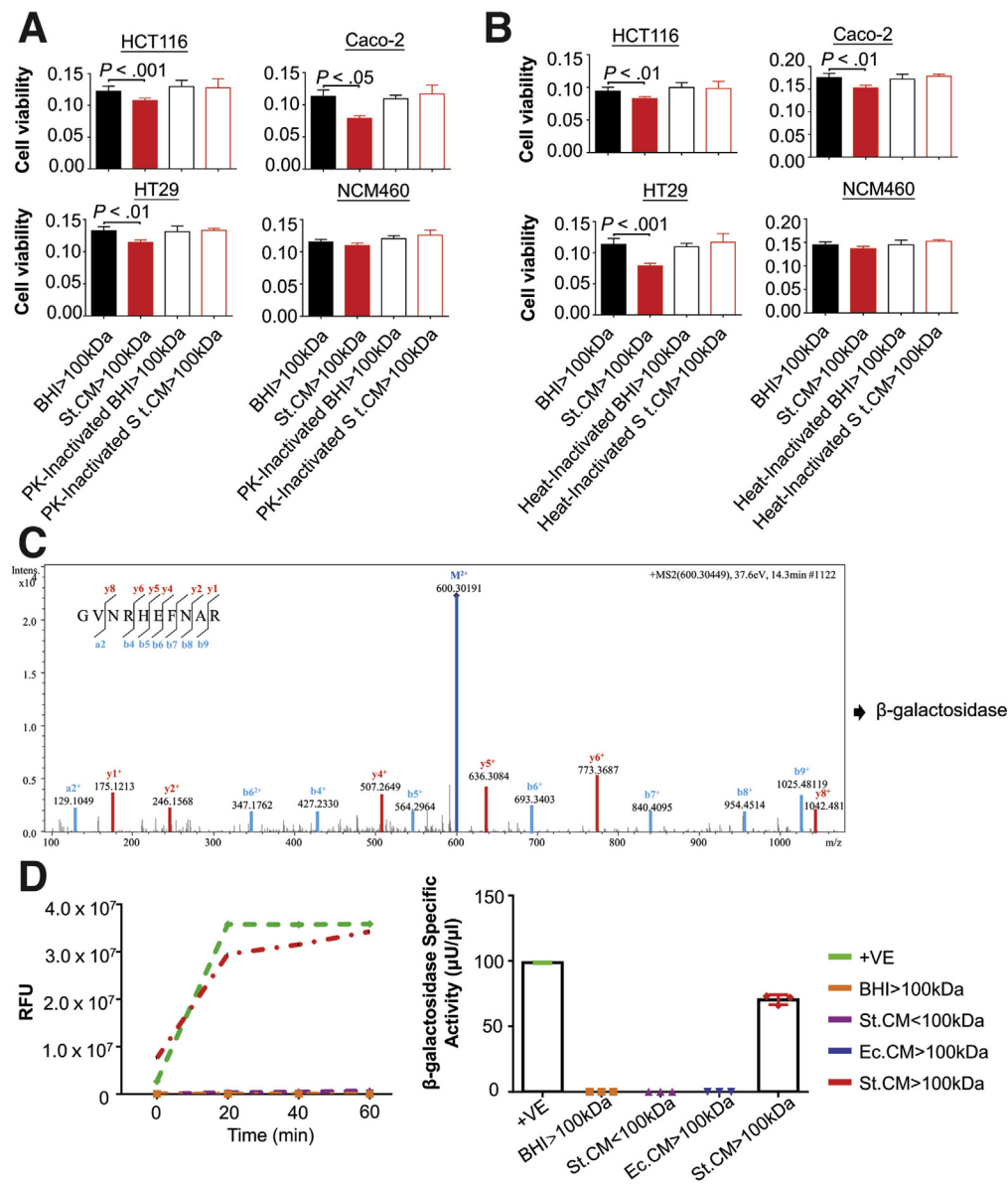


Figure 3. The characterization of the tumor-suppressive molecule secreted by *S. thermophilus* as β-galactosidase. (A) PK-treated St.CM >100-kDa fraction had no effect on CRC cells. (B) Heat-inactivated St.CM >100-kDa fraction had no effect on CRC cells. (C) The St.CM >100-kDa fraction was assessed by 2-dimensional nano-scale liquid chromatography-quadrupole time-of-flight tandem-mass spectrometry, and β-galactosidase was identified as the candidate tumor-suppressive molecule. (D) The activity of β-galactosidase in the St.CM >100-kDa fraction was much higher than the control groups. Data are expressed as mean ± SD. Statistical significance was determined by the Student *t* test. RFU, relative fluorescence units; +VE, positive control.

Streptococcus thermophilus Conditioned Medium >100-kDa Fraction and Galactose Suppress the Hippo Signaling Pathway to Activate Oxidative Phosphorylation

Numerous studies reported that the Hippo-YAP signaling is regulated by intracellular metabolic status.¹³ Given that galactose is transported into cells by means of the same transporters as glucose,¹⁴ we investigated whether St.CM >100 kDa and galactose can interfere with glucose uptake. As shown in Figure 7A, after the treatment of St.CM >100 kDa for 4 hours or galactose for 2 hours, the consumption of 2-(*N*-(7-nitrobenz-2-oxa-1,3-diazol-4-yl)amino)-2-deoxyglucose (2-NBDG) (a fluorescent glucose analog) was reduced significantly in HCT116 cells. The consumption of the glucose was also reduced significantly in the galactose-treated group when the galactose and glucose analog were given simultaneously. However, the reduction

of glucose uptake was not observed in the St.CM >100-kDa-treated group, because St.CM >100 kDa presumably needs time to produce galactose from lactose to inhibit glucose uptake (Supplementary Figure 12A and B). Adenosine 5'-monophosphate-activated protein kinase (AMPK) is the master kinase that senses cellular energy and is required to mediate YAP regulation in response to metabolic and energy stress.¹³ As expected, the reduction of glucose uptake activated AMPK and increased phosphorylation of acetyl-CoA carboxylase (ACC), in agreement with the induction of YAP Ser 127 phosphorylation (Figure 6C, Supplementary Figure 11C). Moreover, the activation of AMPK was observed in tumor tissues isolated from the WT but not the mutant *S. thermophilus*-gavaged mice (Figure 6H).

We then examined the transcription of a panel of glucose metabolism-related genes in cells treated by St.CM >100-kDa, St.CM <100-kDa, or BHI >100-kDa fractions.

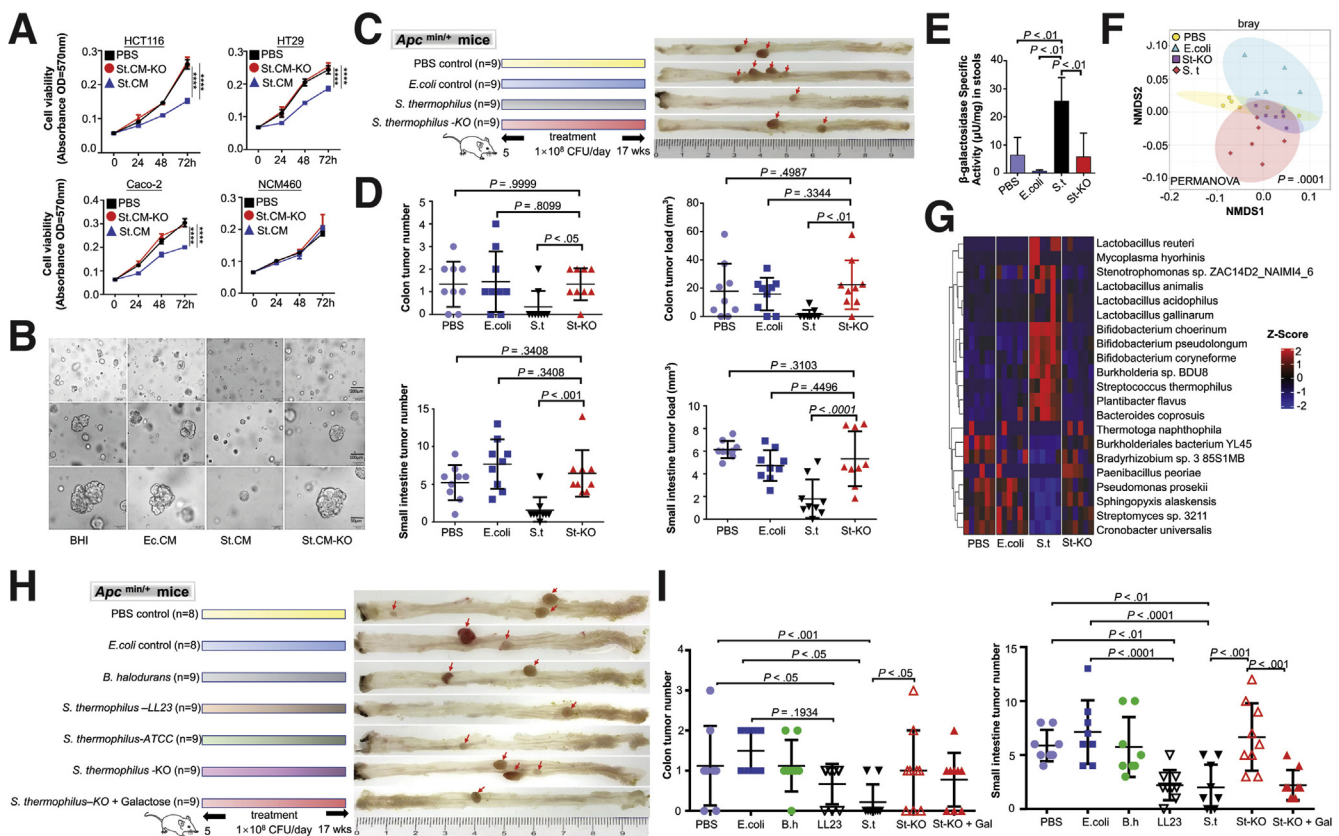


Figure 4. The antitumor effect of *S. thermophilus* is mediated by the secretion of β -galactosidase. The antitumor effects of the St.CM on (A) colon cancer cells and (B) human colon cancer organoids disappeared after LacZ knockout. (C) Schematic diagram shows the experimental design, time line, and representative colonic morphologies of the *Apc*^{min/+} mouse model. (D) The colonic tumor number and tumor load (upper panel) and small-intestine tumor number and tumor load (bottom panel) of *Apc*^{min/+} mice. (E) The overall β -galactosidase activity in stool samples of *Apc*^{min/+} mice. (F) Principal coordinate analysis comparing the microbiome composition in stool samples of *Apc*^{min/+} mice. (G) Heat map representation of β -galactosidase-dependent modulation of bacteria at the species level in *Apc*^{min/+} mice. (H) Schematic diagram shows the experimental design, time line, and representative colonic morphologies of the *Apc*^{min/+} mouse model. (I) Colonic (left panel) and small intestine (right panel) tumor number of *Apc*^{min/+} mice. Data are expressed as mean \pm SD. Statistical significance was determined by 2-way or 1-way ANOVA where appropriate. ***P < .0001. S.t, *Streptococcus thermophilus*; St-KO, *Streptococcus thermophilus* with LacZ knocked out; B.h, *Bacillus halodurans*; LL23, *S. thermophilus* LL23; Gal, galactose.

Transcription of hexokinase 2 (*HK2*), which catalyzes glucose phosphorylation (the rate-limiting first step of glycolysis), was significantly lower in the St.CM >100-kDa-treated group (Supplementary Figure 12C). The down-regulation of *HK2* was validated at mRNA and protein levels in cells treated with St.CM >100 kDa and galactose (Figure 7B and C), and the YAP-dependent expression of *HK2* was confirmed in HCT116 cells, in which the down-regulation of *HK2* was restored by enforced expression of YAP1 (Figure 7C). The depletion of *HK2* was also remarkable in the tumor tissues isolated from the WT *S. thermophilus*-gavaged mice but indiscernible in those administered with the mutant *S. thermophilus* (Figure 6H). A conserved TEAD-binding site in the *HK2* promoter was reported.¹⁵ These findings suggest that metabolic stress-induced inhibition of YAP1 further reinforced the restraint of glucose metabolism.

HK2 is a critical enzyme involved in Warburg glycosis.¹⁶ Depletion of *HK2* can inhibit glycolysis and induce oxidative phosphorylation (OXPHO).¹⁷ Concordantly, our gene set

enrichment analysis of transcriptome profiles revealed that OXPHO was enriched significantly in St.CM >100-kDa-treated HCT116 cells compared with BHI >100 kDa (Figure 7D), in which most of the OXPHO enzyme-encoding genes were upregulated (Supplementary Figure 12D). Accordingly, the maximal, basal oxygen consumption rate, and adenosine 5'-triphosphate production were elevated significantly after the treatment of St.CM >100 kDa (Figure 7E), which was coupled to a significant down-regulation of glycolytic flux in glucose uptake and lactate production (Figure 7F). The same results were observed in galactose-treated HCT116 cells (Figure 7G and H). These results suggested that treatment with St.CM >100 kDa and galactose can shift the metabolism of colon cancer cells from glycolysis to OXPHO.

Discussion

In this study, we validated the depletion of *S. thermophilus* using an orthogonal method. In 2 animal models of

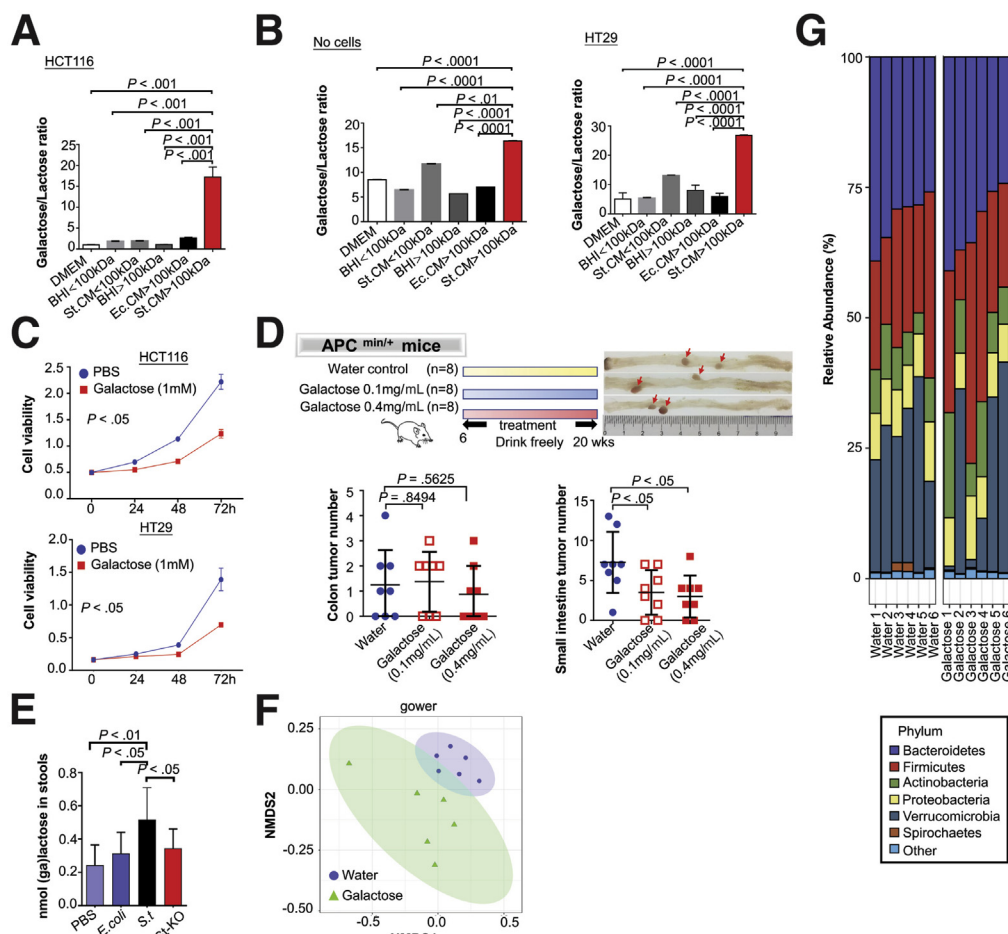


Figure 5. The in vitro and in vivo inhibitory effects of galactose on colon cancer. (A) The galactose-to-lactose ratio in cell culture medium was significantly higher in St.CM >100-kDa-treated cells. (B) The galactose-to-lactose ratio was significantly higher when St.CM >100 kDa was exposed to the cell culture medium even when there were no cells. (C) Galactose reduced CRC cell viability in a time-dependent manner. (D) Schematic diagram shows the experimental design, time line, and representative colonic morphologies of the *Apc^{min/+}* mouse model. Galactose did not affect colonic tumor number while (left panel) but reduced small intestine tumor tumorigenesis (right panel) in *Apc^{min/+}* mice. (E) The galactose content in stool samples of *Apc^{min/+}* mice. (F) Principal coordinate analysis comparing the microbiota composition in stool samples of *Apc^{min/+}* mice. (G) Heat map representation of the modulated bacteria at the phylum level in *Apc^{min/+}* mice. Data are expressed as mean \pm SD. Statistical significance was determined by the Student *t* test or 1-way analysis of variance where appropriate. S.t, *Streptococcus thermophilus*; St-KO, *Streptococcus thermophilus* with *LacZ* knocked out.

colon tumorigenesis, *S thermophilus* significantly lowered tumor number and tumor volume. Moreover, CRC but not normal colonic cell viability was suppressed by *S thermophilus*. Previous studies have already revealed the anti-inflammatory effect of *S thermophilus*¹⁸ and its production of lactate as a signal for modulating colonic epithelium.¹⁹ However, this is the first study to characterize *S thermophilus* as a tumor-suppressive probiotic. Further mechanistic investigation demonstrated the pivotal involvement of β -galactosidase-dependent production of galactose, which inhibited both the Hippo signaling and the Warburg metabolic phenotype in CRC cells.

A key finding of this study is that β -galactosidase from *S thermophilus* functions to prevent tumor formation. *Streptococcus thermophilus* has the capacity to produce β -galactosidase within a very short incubation time.²⁰ Consistent with a previous finding,²¹ we found that *S thermophilus*

remained active in producing β -galactosidase in vivo. Accordingly, the overall β -galactosidase activity increased significantly in fecal samples from the WT *S thermophilus*-gavaged mice (Figure 4E). In addition, we checked The Cancer Genome Atlas data set and found that CRC patients with a higher expression level of *GLB1* (the gene encoding human β -galactosidase) showed a better prognosis (Supplementary Figure 13), indicating that high levels of β -galactosidase generated by the human body or supplemented by probiotics could benefit CRC patients. In contrast to β -galactosidase produced by other mesophilic lactic acid bacteria, which hydrolyze 1 mol of lactose into 4 mol of lactate, *S thermophilus*-derived β -galactosidase only metabolizes the glucose moiety of lactose while it secretes the galactose without fermentation, resulting the production of 2 mol of lactate plus 1 mol of galactose.²² In this regard, the protective effect of fruit and vegetable fibers might be

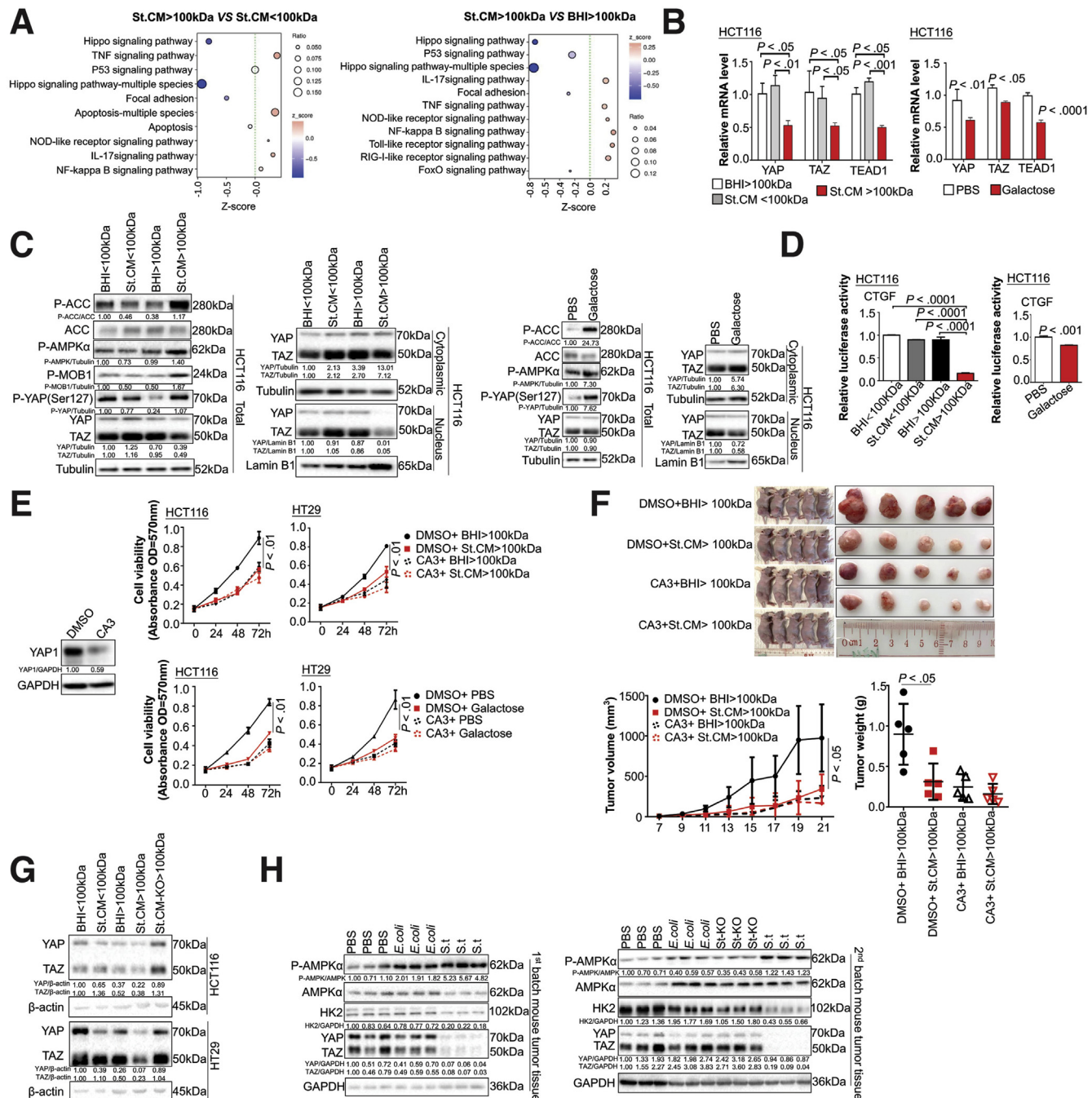


Figure 6. The inhibition of the oncogenic Hippo pathway by St.CM >100 kDa and galactose. (A) Hippo signalling pathway was the top downregulated signalling pathway upon St.CM >100-kDa fraction treatment in HCT116 cells. (B) The mRNA levels of the key genes involved in Hippo signalling pathway were downregulated significantly upon St.CM >100-kDa fraction and galactose (1 mmol/L) treatment in HCT116 cells. (C) St.CM >100-kDa fraction (left panel) and galactose (1 mmol/L) (right panel) increased phosphorylated (P)-AMPK and P-ACC, induced YAP Ser127 phosphorylation, YAP cytoplasmic retention, and blocked YAP nuclear translocation. (D) Relative luciferase assay was performed to validate the downstream transcription factor of the Hippo signalling pathway. (E) Pharmacologic manipulation of the Hippo signalling pathway by CA3 abolished the inhibitory effect of St.CM >100-kDa fraction (upper panel) and galactose (1 mmol/L) (bottom panel) on CRC cell proliferation. (F) CA3 abolished the tumor-suppressive effect of St.CM >100-kDa fraction in the xenograft model. (G) β -Galactosidase mediated the inhibition of the Hippo signalling pathway by *S. thermophilus*. (H) β -Galactosidase mediated the inhibition of the Hippo pathway and the activation of OXPHO by *S. thermophilus* in tumor tissues formed in *Apc*^{min/+} mice (proteins were pooled from each mouse and performed in triplicate). Data are expressed as mean \pm SD. Statistical significance was determined by the Student *t* test or 2-way analysis of variance where appropriate. DMSO, dimethyl sulfoxide; GAPDH, glyceraldehyde-3-phosphate dehydrogenase; IL, interleukin; NF, nuclear factor; S.t, *Streptococcus thermophilus*; St-KO, *Streptococcus thermophilus* with *LacZ* knocked out; TNF, tumor necrosis factor.

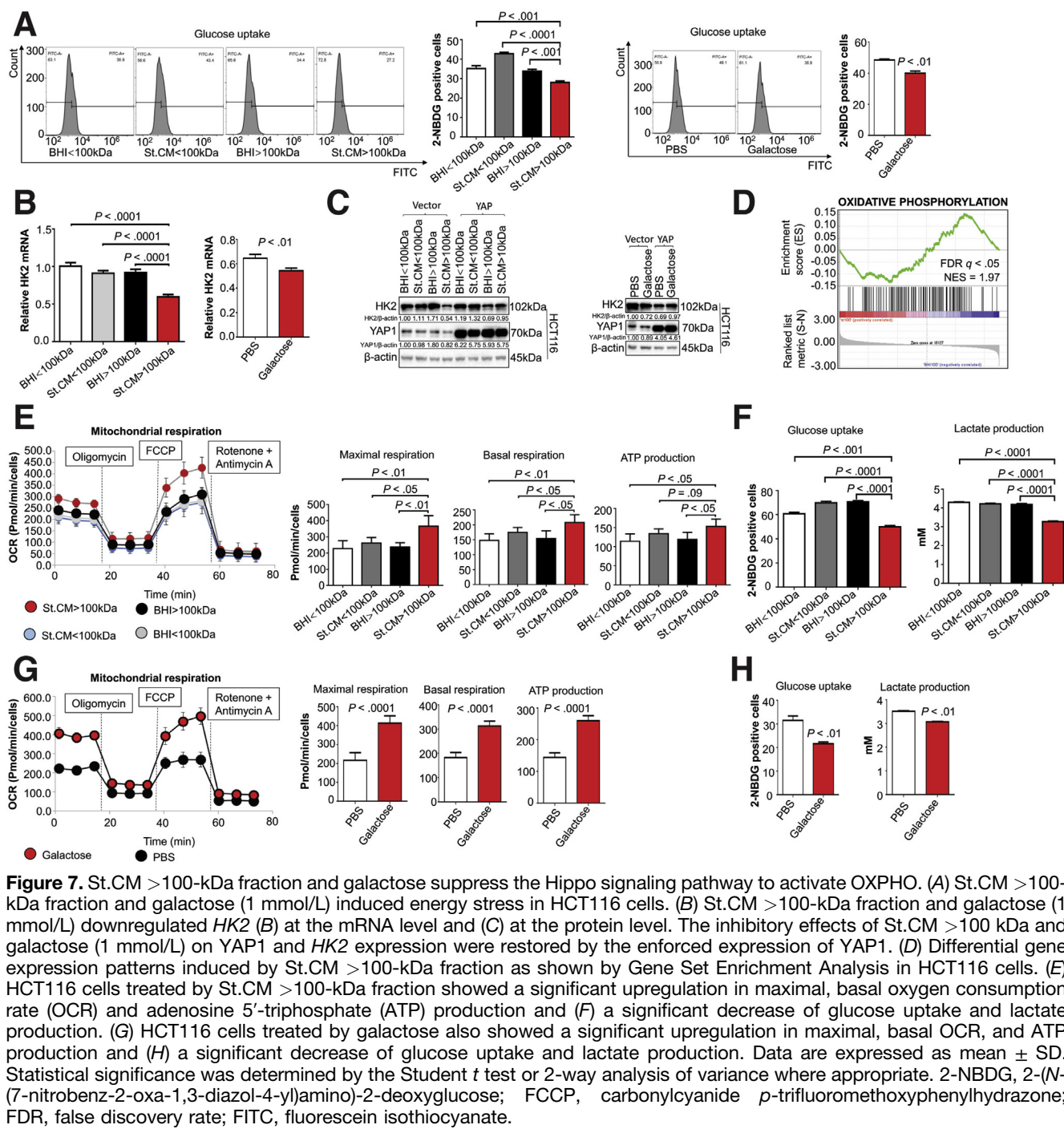


Figure 7. St.CM >100-kDa fraction and galactose suppress the Hippo signaling pathway to activate OXPHO. (A) St.CM >100-kDa fraction and galactose (1 mmol/L) induced energy stress in HCT116 cells. (B) St.CM >100-kDa fraction and galactose (1 mmol/L) downregulated HK2 (B) at the mRNA level and (C) at the protein level. The inhibitory effects of St.CM >100 kDa and galactose (1 mmol/L) on YAP1 and HK2 expression were restored by the enforced expression of YAP1. (D) Differential gene expression patterns induced by St.CM >100-kDa fraction as shown by Gene Set Enrichment Analysis in HCT116 cells. (E) HCT116 cells treated by St.CM >100-kDa fraction showed a significant upregulation in maximal, basal oxygen consumption rate (OCR) and adenosine 5'-triphosphate (ATP) production and (F) a significant decrease of glucose uptake and lactate production. (G) HCT116 cells treated by galactose also showed a significant upregulation in maximal, basal OCR, and ATP production and (H) a significant decrease of glucose uptake and lactate production. Data are expressed as mean \pm SD. Statistical significance was determined by the Student *t* test or 2-way analysis of variance where appropriate. 2-NBDG, 2-(*N*-(7-nitrobenz-2-oxa-1,3-diazol-4-yl)amino)-2-deoxyglucose; FCCP, carbonylcyanide *p*-trifluoromethoxyphenylhydrazone; FDR, false discovery rate; FITC, fluorescein isothiocyanate.

related to their galactose content.²³ Consistently, we found that galactose by itself lowered CRC cell viability in vitro and reduced intestinal tumor number in vivo. Taken together, these data suggested that galactose has a protective effect against CRC.

Lactose intolerance occurs when the β -galactosidase activity in the small intestine is not sufficient. The lactose cannot be digested and thus reaches the colon, causing the symptoms of lactose intolerance. *S thermophilus* can produce β -galactosidase to help digest the extra lactose into galactose, resulting in the reduction of lactose in the

colon. Preliminary epidemiologic evidence indicates lactose intolerance as a possible risk factor for CRC.²⁴ However, further large-cohort studies are warranted to confirm the linkage.

Another striking observation in this study is the β -galactosidase-dependent modulating effect of *S thermophilus* on the gut microbiota. We found that *S thermophilus*, in a β -galactosidase-dependent manner, increased the abundance of other well-known probiotics including the *Bifidobacterium* and *Lactobacillus* spp. Consistently, galactose, a product produced by

β -galactosidase, showed increased abundance of these probiotics. Intriguingly, galactose treatment also decreased the abundance of CRC-enriched pathogenic bacteria, which further suggested the potential involvement of the gut microbiota in mediating the CRC-suppressive effect of galactose. It became evident that *Bifidobacterium* or *Lactobacillus* genera could be used as an adjuvant for cancer prevention by modulating the intestinal microbiota and host immune response.³ It is, therefore, biologically plausible that the beneficial effect of *S thermophilus* on CRC prevention could be mediated, in part, by enhancing the colonization of these probiotics.

The Hippo signaling is an oncogenic pathway with its activation associated with larger tumor size in intestinal tumorigenesis.²⁵ In this study, we found that St.CM >100 kDa and galactose both antagonized glucose uptake and resulted in metabolic stress manifested as increased AMPK and ACC phosphorylation in CRC cells. Both St.CM >100 kDa and galactose also induced YAP S127 phosphorylation and retained YAP in the cytoplasm. These findings recapitulated the known regulation of Hippo signaling by the energy-sensing AMPK pathway.¹³

In the downstream, we discovered that *HK2*, a key mediator of aerobic glycolysis¹⁶ was downregulated significantly in cells treated with St.CM >100 kDa and galactose. Consistently, YAP-regulated expression of *HK2* has been reported in breast cancer.¹⁵ Depletion of *HK2* is known to inhibit glycolysis and induce OXPHO,¹⁶ which are concordant with our observation of the anti-Warburg phenotype produced by St.CM >100 kDa and galactose in CRC cells. Consistently, the energy homeostasis and the Hippo signaling were found to be disrupted in the tumor tissues from mice receiving the WT *S thermophilus*, whereas the mutant *S thermophilus* failed to produce this phenotype. Our finding further verified the involvement of *S thermophilus*-dependent production of β -galactosidase in inhibiting the Hippo oncogenic pathway and the metabolism of tumor cells.

Conclusion

In summary, we demonstrated that *S thermophilus* prevents colon tumorigenesis in animal models. The antitumor effect was mediated by the secretion of β -galactosidase for producing galactose and possibly its synergistic effect with other well-known probiotics. Galactose production then interferes with energy homeostasis and activates AMPK kinase, leading to the phosphorylation of YAP and activation of OXPHO, thus culminating in an anti-Warburg phenotype to inhibit tumorigenesis. Taken together, *S thermophilus* and its secreted molecules are novel prophylactics for CRC prevention.

Supplementary Material

Note: To access the supplementary material accompanying this article, visit the online version of *Gastroenterology* at

www.gastrojournal.org, and at <https://doi.org/10.1053/j.gastro.2020.09.003>.

References

1. Siegel RL, Miller KD, Jemal A. Cancer statistics, 2019. CA Cancer J Clin 2019;69:7–34.
2. Subramanian S, Bobashev G, Morris RJ, et al. Personalized medicine for prevention: can risk stratified screening decrease colorectal cancer mortality at an acceptable cost? Cancer Causes Control 2017;28:299–308.
3. Zhao R, Coker OO, Wu J, et al. Aspirin reduces colorectal tumor development in mice and gut microbes reduce its bioavailability and chemopreventive effects. Gastroenterology 2020;159:969–983.e4.
4. Wong SH, Yu J. Gut microbiota in colorectal cancer: mechanisms of action and clinical applications. Nat Rev Gastroenterol Hepatol 2019;16:690–704.
5. Ambalam P, Raman M, Purama RK, et al. Probiotics, prebiotics and colorectal cancer prevention. Best Pract Res Clin Gastroenterol 2016;30:119–131.
6. Dai Z, Coker OO, Nakatsu G, et al. Multi-cohort analysis of colorectal cancer metagenome identified altered bacteria across populations and universal bacterial markers. Microbiome 2018;6:70.
7. Correa NB, Peret Filho LA, Penna FJ, et al. A randomized formula controlled trial of *Bifidobacterium lactis* and *Streptococcus thermophilus* for prevention of antibiotic-associated diarrhea in infants. J Clin Gastroenterol 2005;39:385–389.
8. Thibault H, Aubert-Jacquin C, Goulet O. Effects of long-term consumption of a fermented infant formula (with *Bifidobacterium breve* c50 and *Streptococcus thermophilus* 065) on acute diarrhea in healthy infants. J Pediatr Gastroenterol Nutr 2004;39:147–152.
9. Tooley KL, Howarth GS, Lynn KA, et al. Oral ingestion of *Streptococcus thermophilus* diminishes severity of small intestinal mucositis in methotrexate treated rats. Cancer Biol Ther 2006;5:593–600.
10. Kang W, Tong JH, Chan AW, et al. Yes-associated protein 1 exhibits oncogenic property in gastric cancer and its nuclear accumulation associates with poor prognosis. Clin Cancer Res 2011;17:2130–2139.
11. Kishimoto Y, Takata N, Jinnai T, et al. Sulindac and a cyclooxygenase-2 inhibitor, etodolac, increase APC mRNA in the colon of rats treated with azoxymethane. Gut 2000;47:812–819.
12. Wang Y, Xu X, Maglic D, et al. Comprehensive molecular characterization of the Hippo signaling pathway in cancer. Cell Rep 2018;25:1304–1317.e5.
13. Wang W, Xiao ZD, Li X, et al. AMPK modulates Hippo pathway activity to regulate energy homeostasis. Nat Cell Biol 2015;17:490–499.
14. Mueckler M, Thorens B. The SLC2 (GLUT) family of membrane transporters. Mol Aspects Med 2013;34:121–138.
15. Gao Y, Yang Y, Yuan F, et al. TNFalpha-YAP/p65-HK2 axis mediates breast cancer cell migration. Oncogenesis 2017;6:e383.

16. Lis P, Dylag M, Niedzwiecka K, et al. The HK2 dependent “Warburg effect” and mitochondrial oxidative phosphorylation in cancer: targets for effective therapy with 3-bromopyruvate. *Molecules* 2016; 21:1730.
17. Mathupala SP, Ko YH, Pedersen PL. Hexokinase-2 bound to mitochondria: cancer’s stygian link to the “Warburg effect” and a pivotal target for effective therapy. *Semin Cancer Biol* 2009;19:17–24.
18. Ogita T, Nakashima M, Morita H, et al. *Streptococcus thermophilus* ST28 ameliorates colitis in mice partially by suppression of inflammatory Th17 cells. *J Biomed Biotechnol* 2011;2011:378417.
19. Rul F, Ben-Yahia L, Chegdani F, et al. Impact of the metabolic activity of *Streptococcus thermophilus* on the colon epithelium of gnotobiotic rats. *J Biol Chem* 2011; 286:10288–10296.
20. Sangwan V, Tomar SK, Ali B, et al. Production of beta-galactosidase from *Streptococcus thermophilus* for galactooligosaccharides synthesis. *J Food Sci Technol* 2015;52:4206–4215.
21. Drouault S, Anba J, Corthier G. *Streptococcus thermophilus* is able to produce a beta-galactosidase active during its transit in the digestive tract of germ-free mice. *Appl Environ Microbiol* 2002;68:938–941.
22. Hickey MW, Hillier AJ, Jago GR. Transport and metabolism of lactose, glucose, and galactose in homofermentative lactobacilli. *Appl Environ Microbiol* 1986; 51:825–831.
23. Evans RC, Fear S, Ashby D, et al. Diet and colorectal cancer: an investigation of the lectin/galactose hypothesis. *Gastroenterology* 2002;122:1784–1792.
24. Kim JW. Lactose intolerance and colorectal cancer. *Ann Coloproctol* 2017;33:157–158.
25. Harvey KF, Zhang X, Thomas DM. The Hippo pathway and human cancer. *Nat Rev Cancer* 2013;13:246–257.

Author names in bold designate shared co-first authorship.

Received December 28, 2019. Accepted September 1, 2020.

Correspondence

Address correspondence to: William K.K. Wu, PhD, Department of Anaesthesia and Intensive Care, The Chinese University of Hong Kong, Hong Kong. e-mail: wukakei@cuhk.edu.hk; Jun Yu, MD, PhD, Department of Medicine and Therapeutics, Prince of Wales Hospital, The Chinese University of Hong Kong, Hong Kong. e-mail: junyu@cuhk.edu.hk; Jian-Lin Wu, PhD, State Key Laboratory of Quality Research in Chinese Medicines, Macau University of Science and Technology, Macao. e-mail: jlwu@must.edu.mo; and Matthew Tak Vai Chan, MBBS, Department of Anaesthesia and Intensive Care, The Chinese University of Hong Kong. e-mail: mtvchan@cuhk.edu.hk.

Acknowledgments

The authors thank Siu Hong Chu (Institute of Digestive Disease, CUHK) for his help with animal experiments.

CRediT Authorship Contributions

Qing Li, MD (Data curation: Lead; Project administration: Lead; Validation: Lead; Writing – original draft: Lead); Wei Hu, PhD (Methodology: Equal); Wei-Xin Liu, MPhil (Data curation: Equal; Formal analysis: Equal); Liu-Yang Zhao, PhD (Methodology: Supporting; Visualization: Supporting); Dan Huang, PhD (Data curation: Supporting; Formal analysis: Supporting); Xiao-Dong Liu, PhD (Methodology: Supporting); Hung Chan, MPhil (Software: Supporting); Yuchen Zhang, MS (Methodology: Supporting); Ju-Deng Zeng, MS (Visualization: Supporting); Olabisi Oluwabukola Coker, PhD (Formal analysis: Supporting); Wei Kang, PhD (Resources: Supporting); Simon Siu Man Ng, MBChB(Hons), MD (Resources: Supporting); Lin Zhang, PhD (Investigation: Supporting); Sunny Hei Wong, MBChB(Hons), DPhil (Resources: Supporting); Tony Gin, MBChB, MD (Investigation: Supporting); Matthew Tak Vai Chan, MBBS, PhD (Supervision: Supporting); Jian-Lin Wu, PhD (Supervision: Supporting); Jun Yu, MD, PhD (Supervision: Equal); William Ka Kei Wu, PhD (Supervision: Equal)

Conflicts of interest

The authors declare that they have no conflicts of interest.

Funding

This project was supported by Science and Technology Program Grant Shenzhen (JCYJ20170413161534162), National Key R&D Program of China (2017YFE0190700), Health and Medical Research Fund (HMRF) Hong Kong (17160862), and Lim Peng Suan Charitable Trust. The study sponsor did not play any role in the study design or in the collection, analysis, and interpretation of data.

Supplementary Materials and Methods

DNA Extraction and *Streptococcus thermophilus* Quantification by Quantitative Polymerase Chain Reaction

Stool samples were placed on ice, and genomic DNAs were extracted following the instruction of ZR Fecal DNA MiniPrep (Zymo Research, Irvine, CA). The isolated DNA was quantified by NanoDrop 2000 spectrophotometer (Thermo Fisher Scientific, Waltham, MA). Amplification and detection of *S thermophilus* were conducted using Universal SYBR Green Master reaction, and the reaction was analyzed by QuantStudio 7 Flex System (Thermo Fisher Scientific). The thermal cycles were 95°C for 10 minutes and 95°C for 15 seconds for 45 cycles, after 60°C for 1 minute. Primers used for *S thermophilus* detection were forward (5'→3') CAGCCATAATGGTGAATCAGT; reverse (5'→3') TTGAG-CATTGCGAACTTGTGA. Primers for total bacteria detection were forward (5'→3') CCTACGGGAGGCAGCAG; reverse (5'→3') ATTACCGCGGCTGCTGGC.

Streptococcus thermophilus Isolation From Human Fecal Samples

Human fecal samples from healthy individuals with a high abundance of *S thermophilus* were used for bacteria isolation. Fecal samples were resuspended in PBS, followed by vibrating for 15 minutes. Residues were removed by filtering the fecal samples through a 100-μm cell strainer (Thermo Fisher Scientific). The filtered samples were spread on M17 agar plate supplemented with 1% lactose and incubated in aerobic conditions at 45°C for 24 hours. The identities of the colonies were determined by Sanger sequencing and confirmed by *S thermophilus*-specific primers.

Bacterial Attachment Assay

The bacteria attachment assay was performed as we described previously.¹ Colon cells (1×10^5 per well) were seeded on 12-well plates and cocultured with *S thermophilus* or mutant *S thermophilus* (multiplicity of infection = 100) under aerobic conditions. After 4 hours, the culture medium was removed, and the cells were washed 5 times with PBS. The cells were then lysed for 5 minutes with 500 μL of cold Triton 1x, and the bacteria were recovered on BHI agar plate at 37°C under aerobic conditions.

Shotgun Metagenomic Analysis

Metagenomic data sets for human fecal samples were obtained as previously described.² Wilcoxon's rank sum test was performed to determine the difference between the abundance of *S thermophilus* in CRC stools and normal control. Shotgun metagenomic sequencing of mice fecal samples were performed on Illumina HiSeq 2000 platform (Illumina, San Diego, CA). Quality control and data analysis were performed as mentioned before. The profile of bacterial taxonomic composition of

metagenomics sequences was constructed using MetaPhiAn pipeline.³

Colorectal Cancer Patient-Derived Organoid Culture

Human tissue biopsy samples were obtained from a 46-year-old woman who was diagnosed with colorectal adenocarcinoma in the Prince of Wales Hospital, The Chinese University of Hong Kong. The samples were processed with the patient's consent. The pathologic specimens were embedded into Matrigel and placed in DMEM/F12 + GlutaMAX (Invitrogen, Carlsbad, CA) containing N2 and B27 supplements (Invitrogen), 10 mmol/L HEPES, 1.25 mmol/L N-acetyl cysteine (Sigma-Aldrich, St Louis, MO), glutamine, 1% penicillin/streptomycin (Sigma-Aldrich), 10 μmol/L SB202190-monohydrochloride (Sigma-Aldrich), R-spondin-1 (RSPO-1), Noggin, WNT3A, and 50 ng/mL epithelial growth factor (Invitrogen). Treatment containing 20% (vol/vol) bacteria CM was added into the culture medium directly. The treatment medium was changed every 3 days.

Characterization of the Antitumor Molecule(s)

The antitumor molecule(s) were digested by PK at 55°C for 2 hours or heat-inactivated at 100°C for 30 minutes. The PK was then inactivated at 95°C for 10 minutes.

Silver Staining and In-Gel Digestion

The antitumor molecule(s) were resolved by sodium dodecyl sulfate-polyacrylamide gel electrophoresis (SDS-PAGE) 5%. Silver staining was performed following the instructions provided by the manufacturer (Thermo Scientific, Rockford, IL). After staining, specific bands from the >100-kDa fraction were excised by pipette tips into 1.5 mL plastic tubes for in-gel digestion following the manufacturer's instructions (Thermo Scientific). The obtained peptide mixtures analyzed with mass spectrometry (MS).

Two-Dimensional Nano-Scale Liquid Chromatography-Quadrupole Time-of-Flight Tandem-Mass Spectrometry

The 2-dimensional nano-scale liquid chromatography-quadrupole time-of-flight tandem-MS (2D-nanoLC-Q-TOF/MS) experiments were performed with an Ultimate high-performance LC (HPLC) pump. First, 20 μg of tryptic peptides were loaded onto a strong cation-exchange column (PolySULFOETHYL ATM, 0.3 × 100 mm) and eluted successively by a series of ammonium acetate elutions with the concentrations of 5, 10, 25, 50, and 100 mmol/L at pH 2.7. The volume of each elution was 20 μL. Each eluate from the strong cation-exchange column was transferred to C18 trap column and further desalted with solution A (0.1% trifluoroacetic acid [FA] in 2% HPLC grade acetonitrile [CAN]) at 5 μL/min for 30 minutes. Finally, the desalted fractions were separated in a C18 analytical column at 300 nL/min using (A) 0.1% FA in water and (B) 0.1% FA in ACN with the following gradient: 0 to 30 minutes, 5% B; 30 to 120 minutes, linearly increased B from 5% to 15%; 120 to 140

minutes, linearly increased B from 15% to 50%; 140 to 150 minutes, linearly increased B from 50% to 80%. MS spectral data were processed using the Bruker Compass Data Analysis software (Bruker, Billerica, MA), and the generated peak lists were converted into the Mascot search engine against the Swiss-Prot 51.6 database. Trypsin was selected as an enzyme. $P < .05$ was defined as statistically significant, and β -galactosidase was identified as the potential functional protein. The β -galactosidase from the *E coli* overproducer was obtained from (Sigma-Aldrich) and was used as a positive control.

Colony Formation Assay

Colon cells (1,000 per well) were seeded on 6-well plates, followed by treatment with St.CM (1% St.CM in DMEM). BHI and *Escherichia coli* CM were used as the control. The treatment medium was changed every 3 days. After culturing for 14 to 18 days, cells were fixed with 70% ethanol and stained with 0.5% crystal violet solution. The colony with more than 50 cells was counted. All experiments were performed 3 times in triplicate.

Ki-67 Immunofluorescence Staining

Cell proliferation was assayed by immunofluorescence staining with the anti-Ki-67 antibody (ab833; Abcam, Cambridge, United Kingdom). Negative controls were run by replacing the primary antibody with nonimmune serum. The proliferation index was determined by counting the numbers of positively stained cells as the percentage of the total number of tumor cells. At least 1000 tumor cells were counted each time.

Flow Cytometry

For cell cycle analysis, the treated cells were fixed by 70% ethanol overnight. Cells were then stained with 50 $\mu\text{g}/\text{mL}$ propidium iodide (PI) (BD Pharmingen, San Jose, CA) for 30 minutes at 4°C in the dark. Ten thousand cells were counted by FACSaria cell sorter (BD Biosciences, Franklin Lakes, NJ), and cell cycle profiles were analyzed by the ModFit 3.0 software (Verity Software House, Topsham, ME). The proportion of apoptotic cells was evaluated using the annexin V apoptosis assay. The treated cells were collected and resuspended in 100 μL annexin-binding buffer (10 mmol/L HEPES, 140 mmol/L NaCl, and 2.5 mmol/L CaCl₂, pH 7.4) containing 5 μL of annexin V conjugated with allophycocyanin and 50 $\mu\text{g}/\text{mL}$ PI. After incubation for 15 minutes at room temperature, cells were mixed with an additional 400 μL of ice-cold annexin-binding buffer and analyzed using the FACSaria cell sorter.

RNA Sequencing

Total RNAs were extracted from cells treated with BHI >100 kDa, St.CM <100 kDa, and St.CM >100 kDa (1% vol/vol) using Trizol Reagent (Life Technologies). Three biological replicates were performed for each studied condition. TruSeq Stranded Total Sample Preparation Kit (Illumina) was used for sequencing library construction. Libraries were fed into HiSeq machines according to activity

and expected data volume. RNA sequence reads were mapped to reference genome of *Homo sapiens* GRCh37/hg19. Differentially expressed gene levels were measured by transcript abundance.

Glucose Uptake Assay

Cells (500,000 per well) were seeded in 6-well plates overnight after the treatment for the desired time. The treatment medium was then changed into glucose-free DMEM and 50 $\mu\text{mol}/\text{L}$ 2-(N-(7-nitrobenz-2-oxa-1,3-diazol-4-yl)amino)-2-deoxyglucose (2-NBDG; Invitrogen) was added into cells. After incubation for 1 hour, cells were washed with ice-cold PBS twice, and glucose uptake ability was quantified by using flow cytometry.

Lactate Production Assay

Cells (500,000 per well) were seeded in 6-well plates, followed by the treatment of St.CM >100-kDa fraction and galactose for 72 and 48 hours, respectively. After the treatment, the cells were homogenized in the lactate assay buffer, and all of the procedures were performed following the manufacturer's instruction (BioVison, Milpitas, CA).

Agilent Seahorse XF Cell Mito Stress Test

HCT116 cells (2000 per well) were plated to 96-well Seahorse XF Cell Culture Microplate overnight before the treatment. All the procedures were performed following the manufacturer's instruction (Agilent Technologies, Santa Clara, CA). The concentration of carbonylcyanide *p*-trifluoromethoxyphenylhydrazone (FCCP) used in this experiment was 1.0 $\mu\text{mol}/\text{L}$.

Western Blotting Analysis

Total protein was isolated and separated by SDS-PAGE (6%-12%). The protein in SDS-PAGE was then transferred onto polyvinylidene difluoride membranes (EMD Millipore, Billerica, MA) for approximately 1 to 2 hours, which was then blocked with 10% nonfat milk in 0.05% Tris-based saline-Tween 20 for 2 hours at room temperature. The membrane was incubated with primary antibodies overnight at 4°C and then with secondary antibody at room temperature for 1 hour. The protein band intensities were detected by ECL Plus Western Blotting Detection Reagents (GE Healthcare, Waukesha, WI).

Luciferase Assays

The connective tissue growth factor (CTGF) transcription factor plasmid was a gift from Professor Wei Kang, Department of Anatomical and Cellular Pathology, the Chinese University of Hong Kong. A 600-base pair from the transcription starting site of CTGF was subcloned into the reporter gene vector pGL3-Basic (Promega, Madison, WI). The firefly luciferase construct was cotransfected with the *Renilla* luciferase vector (Promega) control into the cells. At 6 hours after the transfection, the whole medium was changed, and the transfected cells were treated by St.CM >100 kDa or galactose. Dual-Luciferase Reporter Assay

System (Promega) was used to check the luciferase activity after 24 hours of treatment.

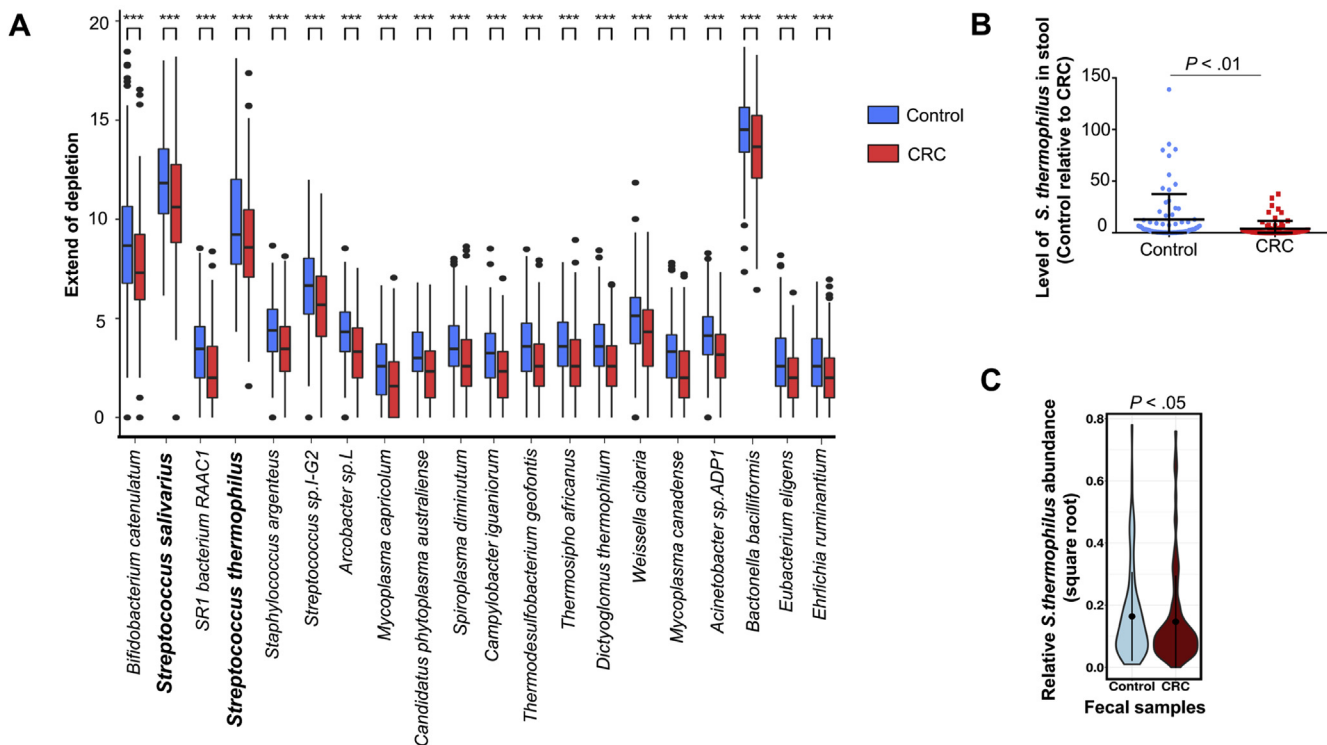
Gene Expression Profiling From RNA Sequencing in The Cancer Genome Atlas Data Set

The full clinical data set in relation to *GLB1* expression levels in CRC and the relationship between *S thermophilus* and YAP1 target genes were downloaded and assessed from The Cancer Genome Atlas Research Network data portal (Illumina HiSeq percentile). This study meets the publication guidelines provided by The Cancer Genome Atlas. <http://cancergenome.nih.gov/publications/publicationguidelines>.

References

1. Long X, Wong CC, Tong L, et al. *Peptostreptococcus anaerobius* promotes colorectal carcinogenesis and modulates tumour immunity. *Nat Microbiol* 2019;4:2319–2330.
2. **Dai Z, Coker OO, Nakatsu G**, et al. Multi-cohort analysis of colorectal cancer metagenome identified altered bacteria across populations and universal bacterial markers. *Microbiome* 2018;6:70.
3. Zhao R, Coker OO, Wu J, et al. Aspirin reduces colorectal tumor development in mice and gut microbes reduce its bioavailability and chemopreventive effects. *Gastroenterology* 2020;159:969–983.e4.

Author names in bold designate shared co-first authorship.



Supplementary Figure 1. *Streptococcus thermophilus* is depleted in stool samples of patients with CRC. (A) The abundance of the CRC-depleted bacteria species with the largest fold change in our previous combined metagenomic data set.⁸ Bold characters are known probiotics. The horizontal line in the middle of each box indicates the median; the top and bottom borders of the box mark the 75th and 25th percentiles, respectively, the whiskers mark the 90th and 10th percentiles, and the circles indicate outliers. (B) Quantitative PCR was used to confirm the abundance of *S. thermophilus* in clinical stool samples from normal controls ($n = 78$) and patients with CRC ($n = 78$). (C) The abundance of *S. thermophilus* in our in-house shotgun metagenome sequencing data from 202 normal individuals and 183 CRC patients. Each spot represents 1 individual. The black dot represents the median, the gray line represents the 95% confidence interval, the wider sections represent a higher probability that members of the population will take on the given value, and the thinner sections represent a lower probability. Statistical significance was assessed by the Student *t* test. *** $P < .001$.

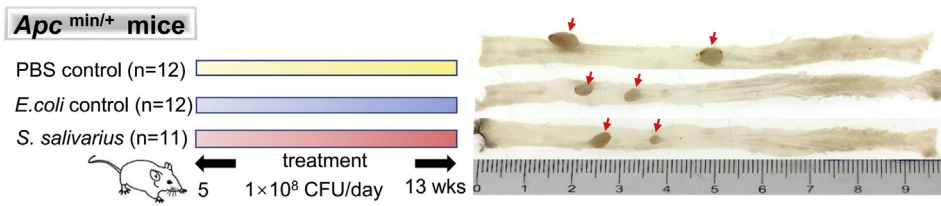
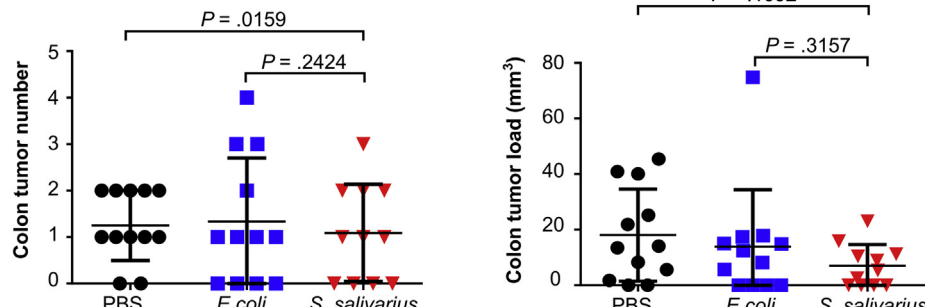
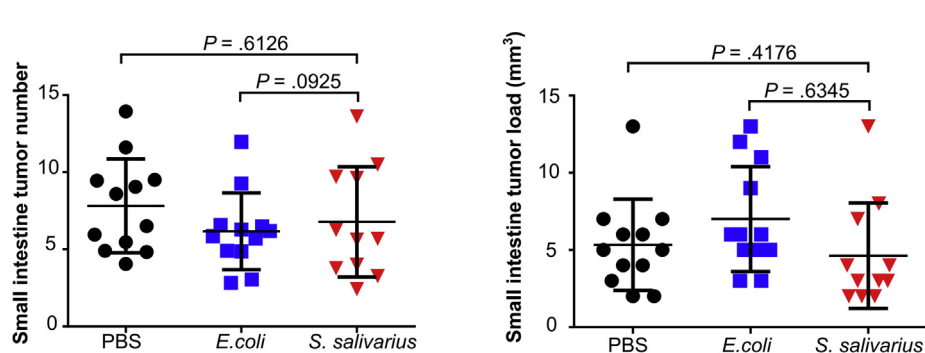
A**B****C****Supplementary**

Figure 2. *Streptococcus salivarius* cannot reduce intestinal tumorigenicity in mice. (A) Schematic diagram shows the experimental design, time line, and representative colonic morphologies of the *Apc*^{min/+} mouse model under different treatment. (B) Colonic tumor number and tumor load of *Apc*^{min/+} mice under different treatments. *Streptococcus salivarius* had no effect on colon tumor number and colon tumor load. (C) Small-intestine tumor number and tumor load of *Apc*^{min/+} mice under different treatments. *Streptococcus salivarius* had no effect on colon tumor number and colon tumor load. Results are presented as mean \pm SD. Statistical significance was determined by 1-way analysis of variance.

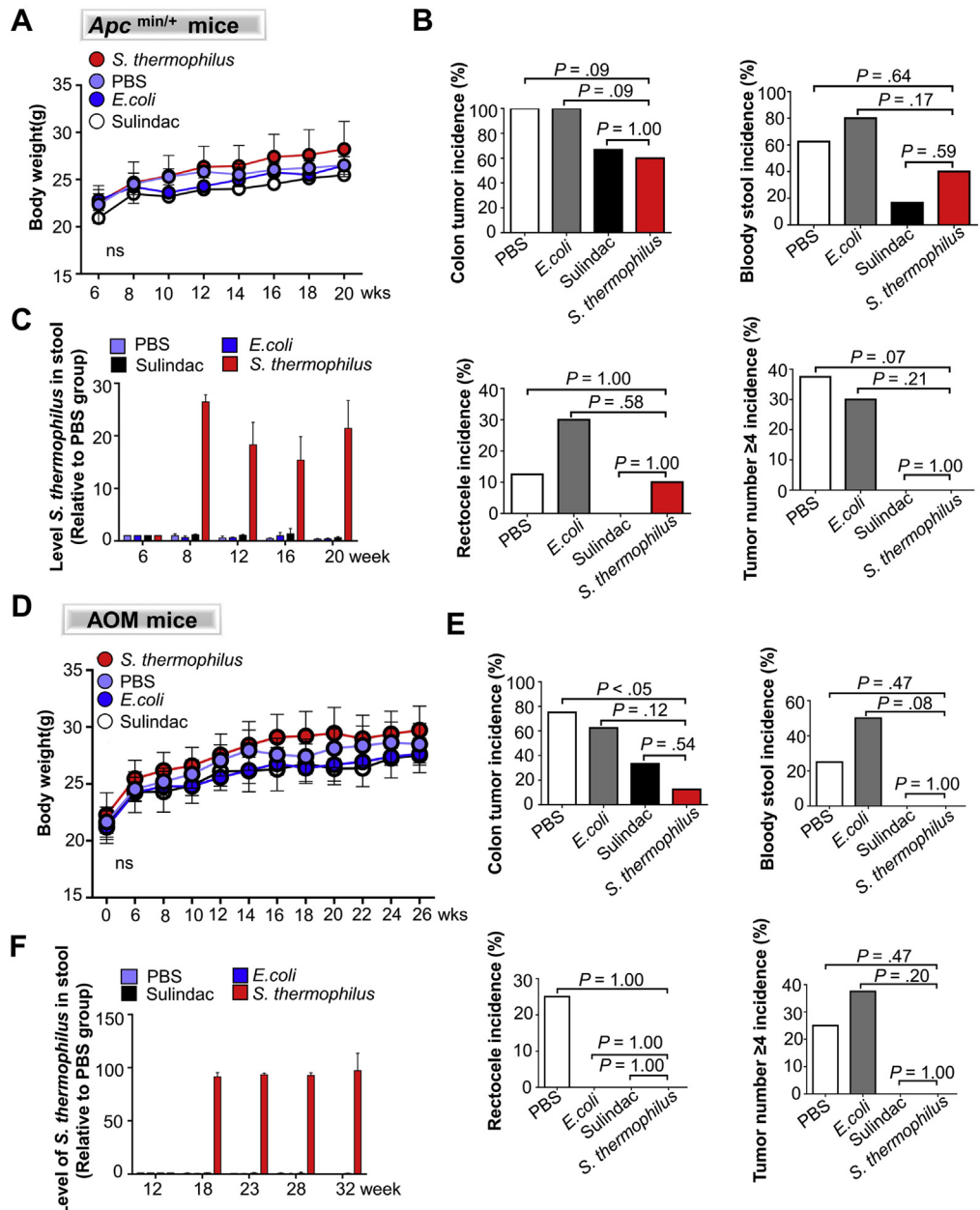
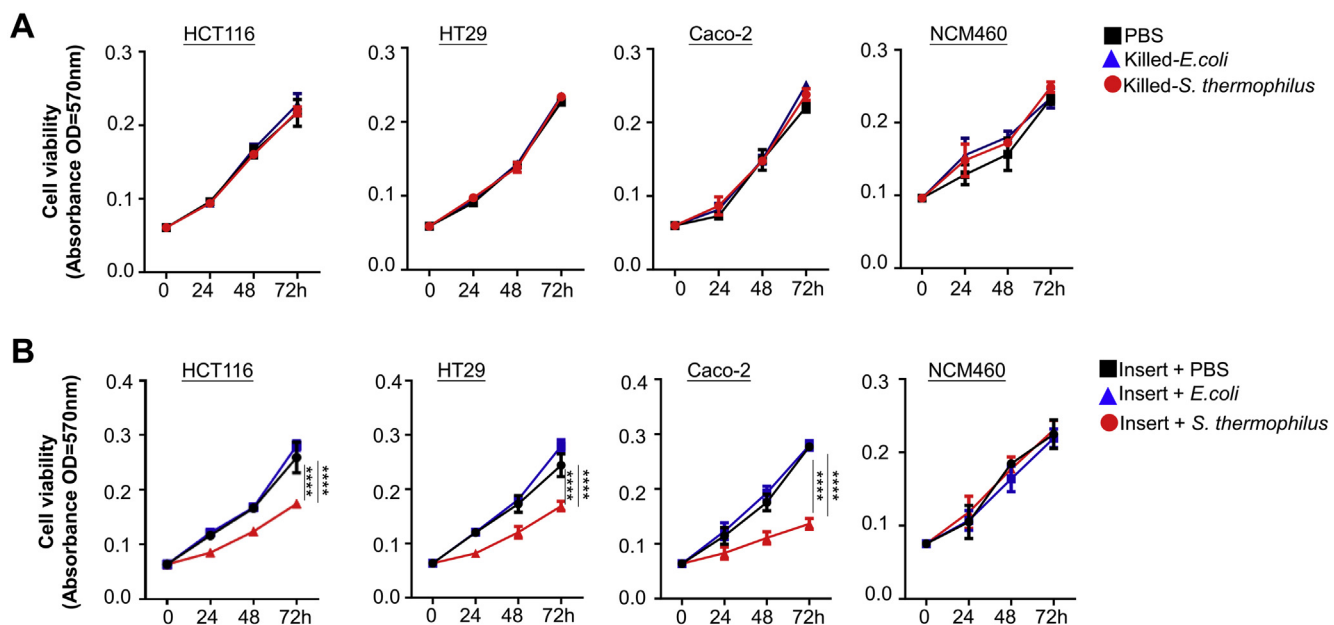
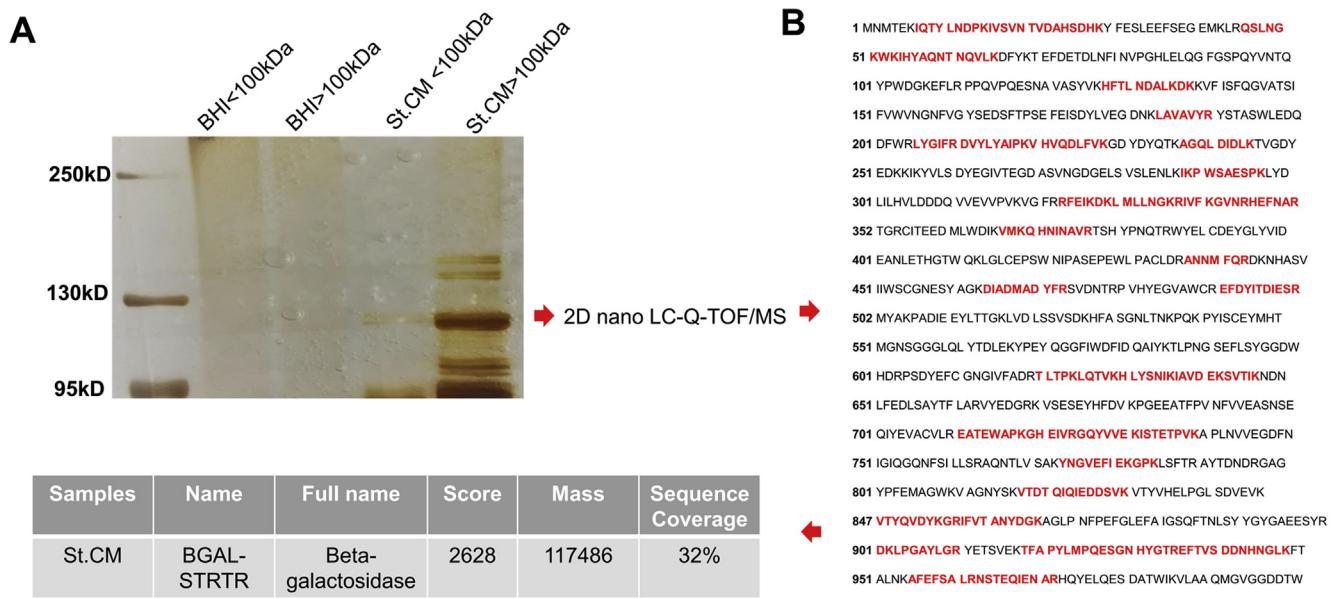
**Supplementary**

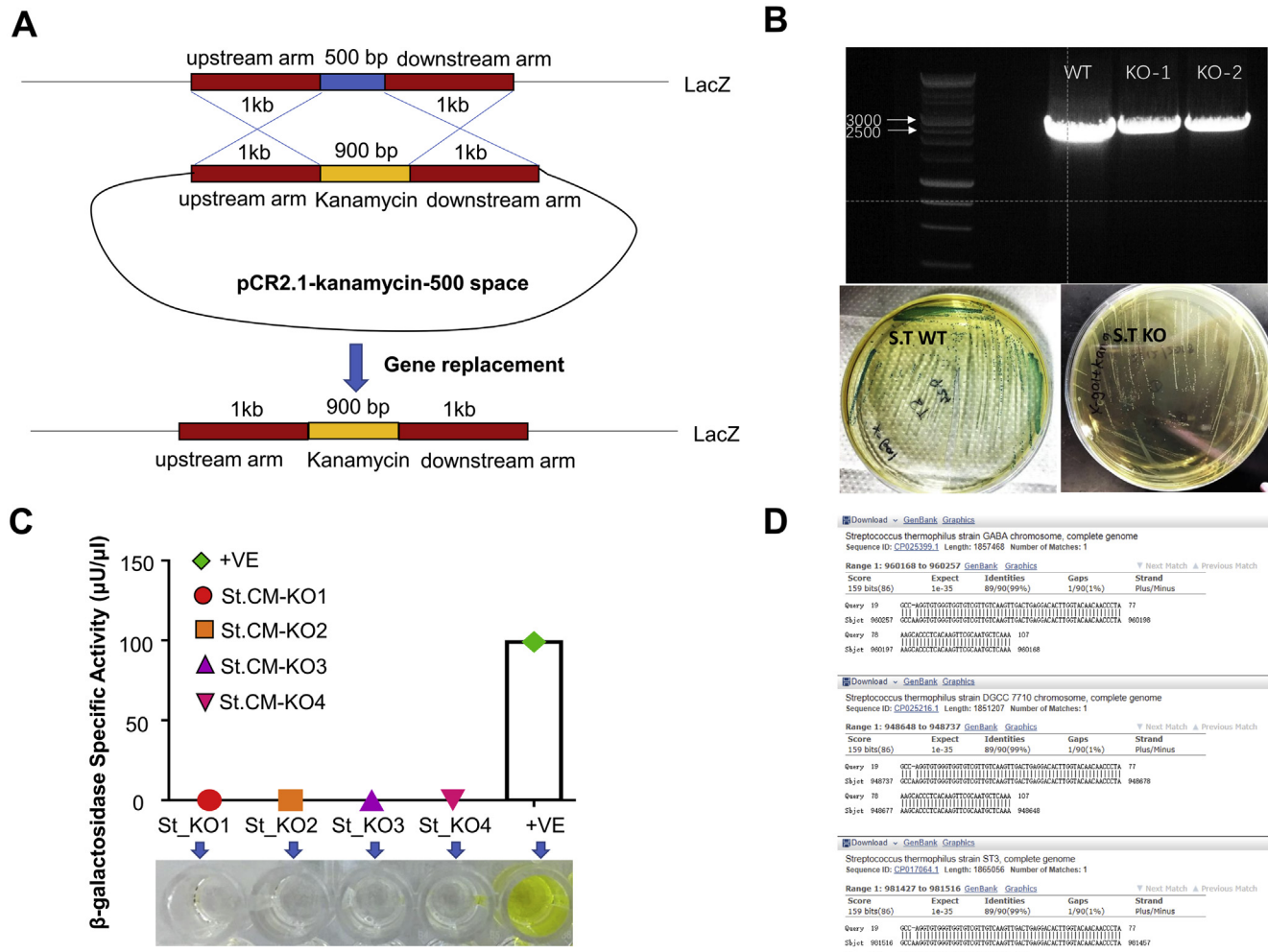
Figure 3. The effects of *S. thermophilus* in mice. (A) The body weight of the *Apc^{min/+}* mice was not affected by the administration of *S. thermophilus*. (B) The symptomatic manifestation of CRC showed a decreasing trend in *S. thermophilus*-fed *Apc^{min/+}* mice. (C) The level of *S. thermophilus* in stool samples of *Apc^{min/+}* mice under different treatments. (D) The body weight of the AOM-induced CRC mice was not affected by the administration of *S. thermophilus*. (E) The symptomatic manifestation of CRC showed a decreasing trend in the *S. thermophilus*-fed AOM-injected mice. (F) The level of *S. thermophilus* in stool samples of the AOM-induced CRC mouse model under different treatments. Statistical significance was determined by χ^2 test or 2-way analysis of variance, where appropriate.



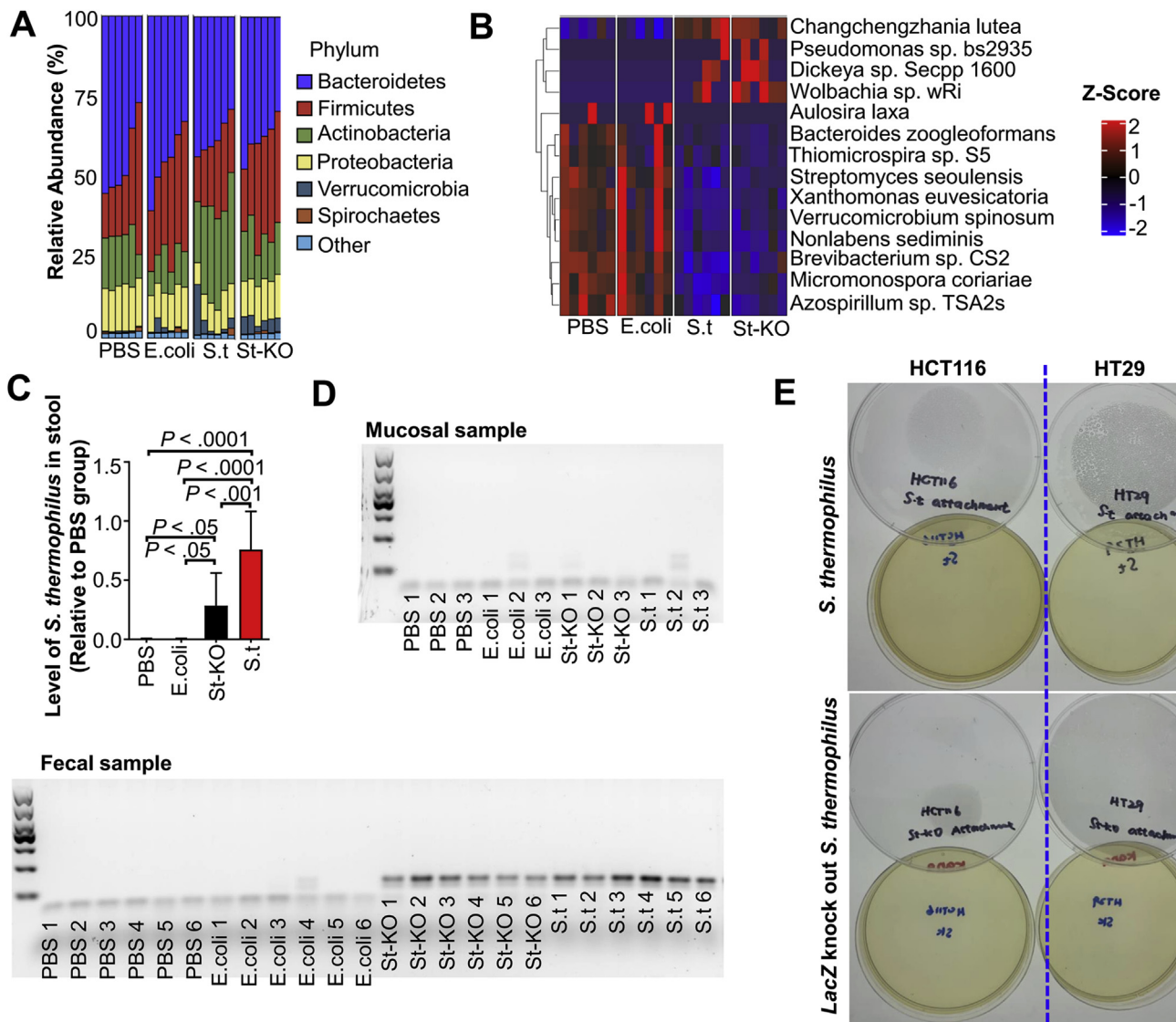
Supplementary Figure 4. The tumor-suppressive effect of *S. thermophilus* is mainly mediated by its secreted molecule(s). (A) Autoclave-killed *S. thermophilus* had no effect on the viability of colon cancer cells. (B) Molecules secreted from *S. thermophilus* diffused from the upside of the transwell insert reduced the cell viability of colon cancer cells but not the normal colon epithelial cells as determined by MTT assay. Data are expressed as mean \pm SD. Statistical significance was determined by 2-way analysis of variance. **** P < .0001.



Supplementary Figure 5. Characterization of the *S. thermophilus*-secreted tumor-suppressive molecule(s). (A) The St.CM >100-kDa fraction was separated by sodium dodecyl sulfate-polyacrylamide gel electrophoresis, and specific bands underwent identification by (B) mass spectrometry. β -Galactosidase was identified. 2D nano LC-Q-TOF/MS, two-dimensional nano-scale liquid chromatography-quadrupole time-of-flight tandem-mass spectrometry.



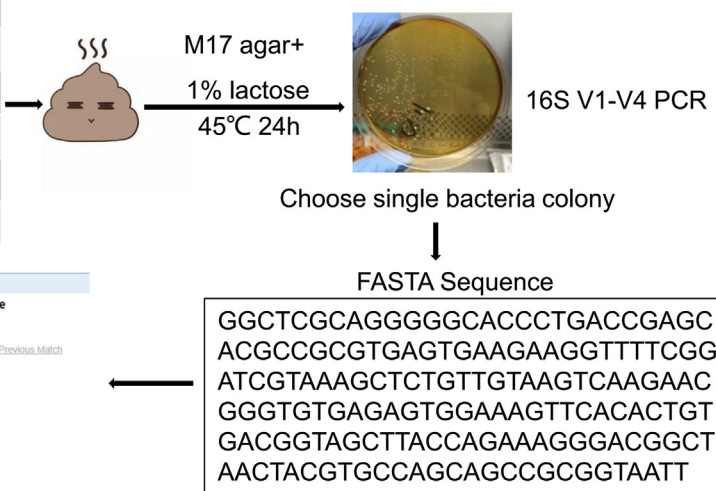
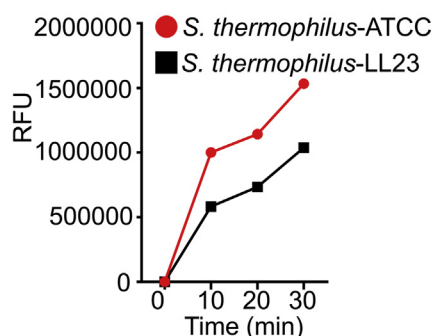
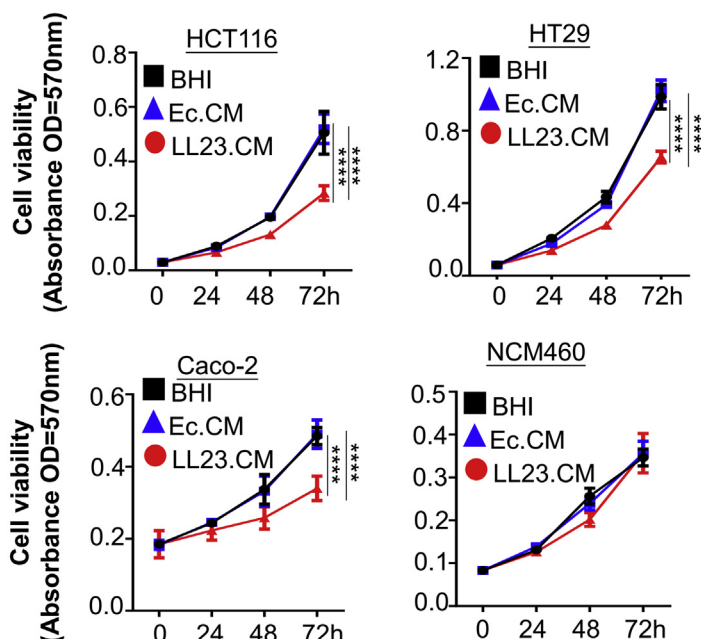
Supplementary Figure 6. The construction of *S. thermophilus* mutant strain. (A) Workflow for the homologous recombination process. (B) PCR was performed for the validation of the successful insertion of the kanamycin resistance gene to *LacZ* (*top panel*), and blue-white screen (*bottom panel*) was used to validate the successful knockout of *LacZ* in *S. thermophilus*. (C) The activity of β -galactosidase activity was abolished. (D) The mutant strain was confirmed to be *S. thermophilus* by 16S ribosomal RNA gene sequencing. GABA, γ -aminobutyric acid.



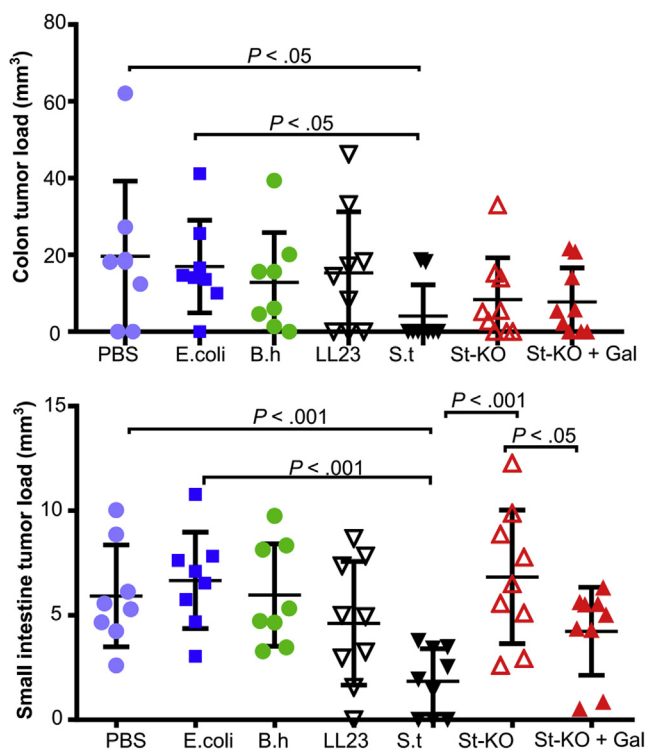
Supplementary Figure 7. The impact of *S. thermophilus* colonization on the gut microbiota. (A) Heat map representation of the modulated bacteria at the phylum level in *Apc*^{min/+} mice under different treatments. (B) Heat map representation of β -galactosidase-independent modulation of bacteria at the species level in *Apc*^{min/+} mice under different treatments. (C) The colonization of *S. thermophilus* in the stool samples of *Apc*^{min/+} mice under different treatments. (D) The colonization of *S. thermophilus* in the mucosal tissue samples of *Apc*^{min/+} mice under different treatments. (E) The attachment ability of WT *S. thermophilus* and mutant *S. thermophilus* in vitro. Data are expressed as mean \pm SD. Statistical significance was determined by 1-way analysis of variance. S.t, *S. thermophilus*; St-KO, *S. thermophilus* with *LacZ* knocked out.

A

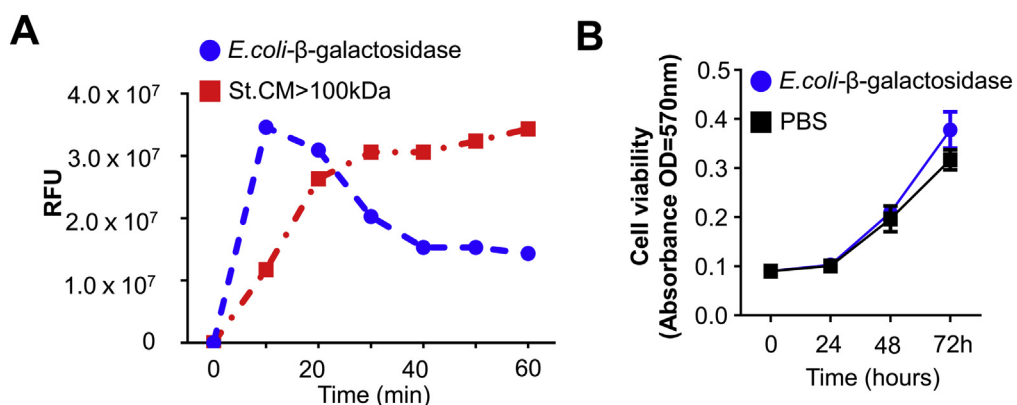
No. of patients	Disease status	<i>S. thermophilus</i> level in stool
Donor 1	Healthy	0.01
Donor 2	Healthy	0.01
Donor 3	Healthy	1.01
Donor 4	Healthy	0.06
Donor 5	Healthy	0.28
Donor 6	Healthy	0.14

**B****C**

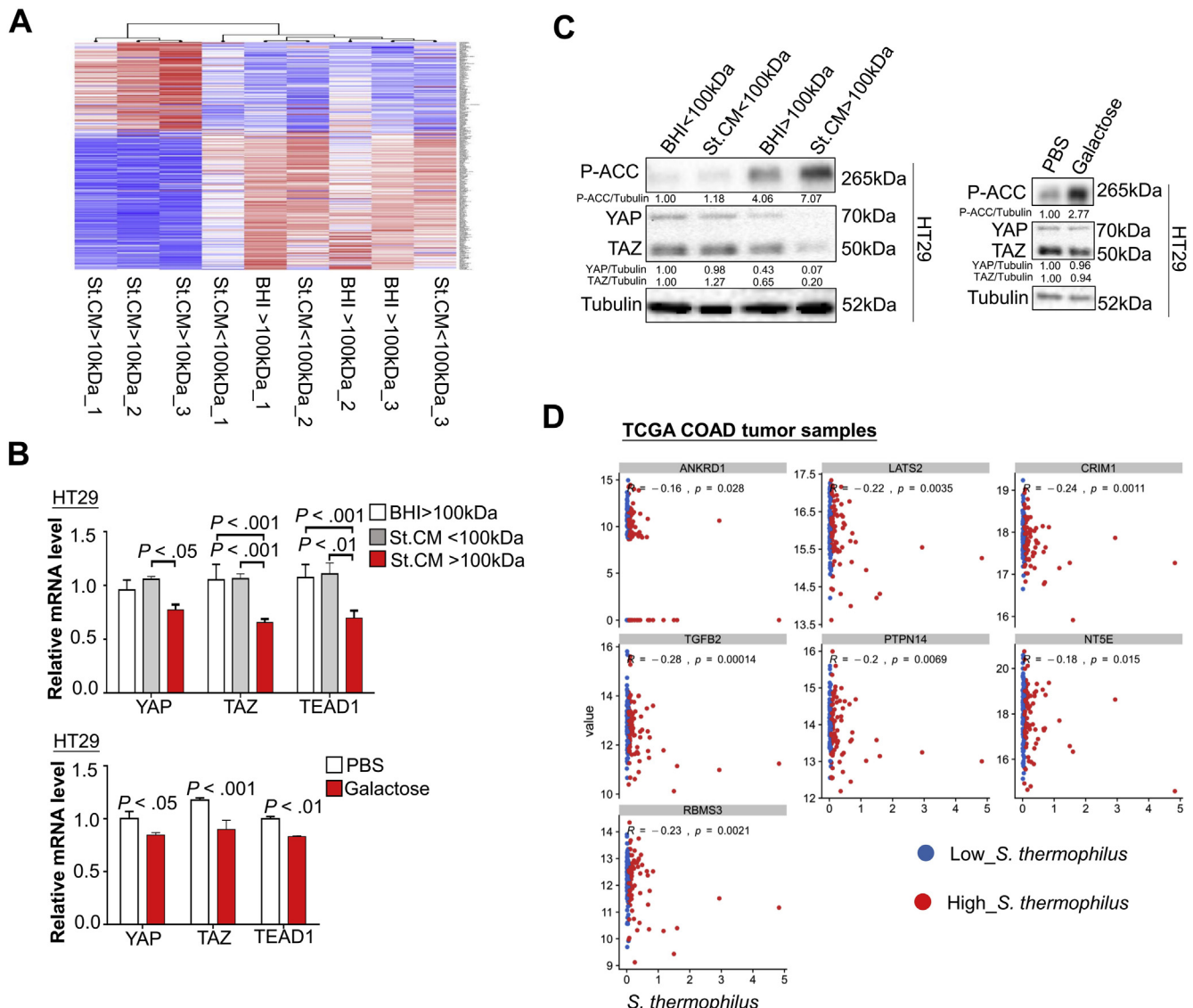
Supplementary Figure 8. Isolation and confirmation of the tumor-suppressive effect of *S thermophilus* from healthy human fecal samples. (A) Schematic diagram shows the isolation workflow. Selection of stool samples with a comparatively high relative abundance of *S thermophilus* from healthy subjects (upper panel). The bacteria colonies were confirmed by cellular morphology and PCR amplification of the phylogenetic marker gene. BLAST results showed the successfully isolated *S thermophilus* LL23 strain from donor 3 (bottom panel). (B) The β -galactosidase activity in different *S thermophilus* strains. RFU, relative fluorescence units. (C) LL23.CM (15%) reduced the colonic cell viability, except NCM460. *Escherichia coli* CM and BHI were used as control. Data are expressed as mean \pm SD. Statistical significance was determined by 2-way analysis of variance. LL23.CM, the conditioned medium of *S thermophilus* LL23 strain.



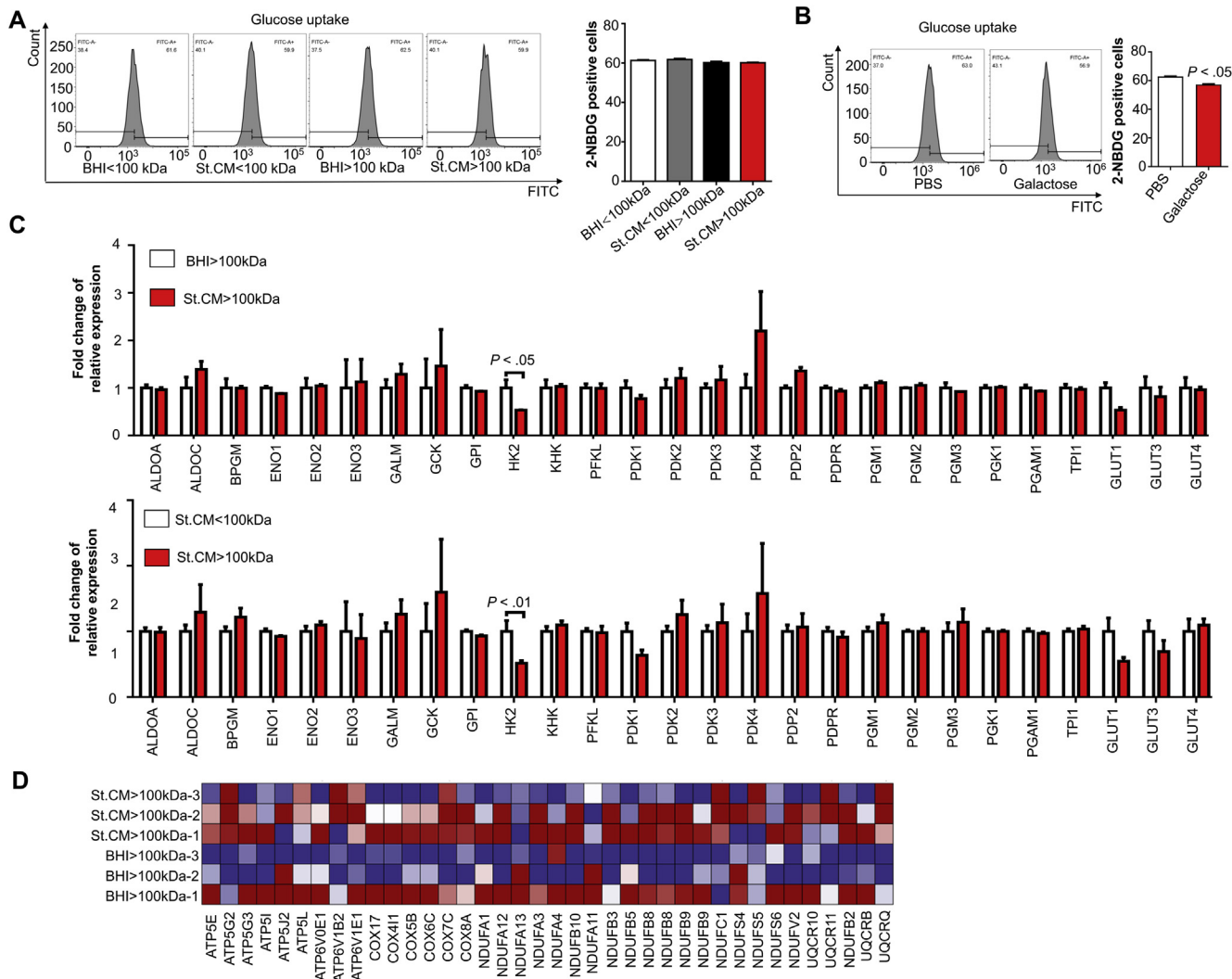
Supplementary Figure 9. The antitumor effect of *S. thermophilus* is mediated by the secretion of β -galactosidase. Colonic (upper panel) and small intestine (lower panel) tumor load of *Apc*^{min/+} mice under different treatments. Data are expressed as mean \pm SD. Statistical significance was determined by 2-way or 1-way analysis of variance, where appropriate. S.t, *S. thermophilus*; St-KO, *S. thermophilus* with LacZ knocked out; B.h, *B. halodurans*; LL23, *S. thermophilus* LL23; Gal, galactose.



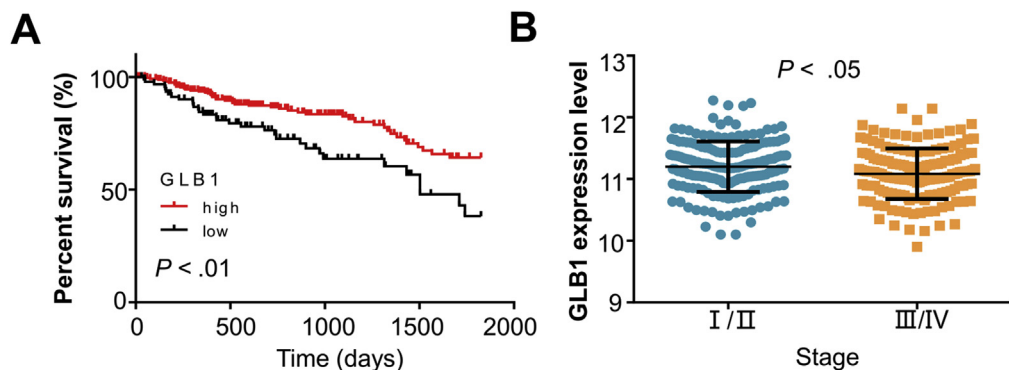
Supplementary Figure 10. The characterization of β -galactosidase from the *E. coli* overproducer. (A) β -Galactosidase derived from the *E. coli* overproducer was not stable. The β -galactosidase in St.CM > 100-kDa fraction remained active throughout the reaction, whereas the activity of *E. coli*-derived β -galactosidase decreased over time. RFU, relative fluorescence units. (B) The β -galactosidase from *E. coli* had no inhibitory effect on CRC cell viability. Data are expressed as mean \pm SD. Statistical significance was determined by 2-way analysis of variance.



Supplementary Figure 11. St.CM >100-kDa fraction and galactose suppress the Hippo signaling pathway. (A) Differential gene expression pattern induced by St.CM >100-kDa fraction as shown by RNA sequencing in HCT116 cells. (B) The inhibition of Hippo signaling was validated at mRNA and (C) protein levels in HT29 cells. P-, phosphorylated. (D) The abundance of *S. thermophilus* had a negative correlation with most of the TAZ/TAZ target genes in The Cancer Genome Atlas Colon Adenocarcinoma (TCGA COAD) cohort (median was used to define high or low *S. thermophilus* in CRC patients). Data are expressed as mean \pm SD. Statistical significance was determined by 1-way analysis of variance.



Supplementary Figure 12. St.CM >100-kDa fraction and galactose induce energy stress and downregulate HK2 transcription. (A) Simultaneous treatment of HCT116 cells with St.CM >100-kDa fraction and glucose analog had no effect on glucose uptake. (B) Simultaneous treatment of HCT116 cells with galactose and glucose analog decreased glucose uptake. (C) St.CM >100-kDa fraction downregulated the transcription of HK2. (D) Heat map shows multiple enzymes involved in OXPHO were enriched and upregulated after treatment with St.CM >100-kDa fraction. Data are expressed as mean \pm SD. Statistical significance was determined by 1-way analysis of variance or the Student *t* test where appropriate.



Supplementary Figure 13. *GLB1* expression levels are associated with CRC prognosis. (A) Kaplan-Meier curve shows that decreased expression of *GLB1* mRNA was associated with poor survival in CRC patients in The Cancer Genome Atlas cohort. (B) *GLB1* levels were higher in early-stage CRC compared with late-stage CRC. Statistical significance was determined by the Student *t* test.